General Disclaimer

One or more of the Following Statements may affect this Document

- This document has been reproduced from the best copy furnished by the organizational source. It is being released in the interest of making available as much information as possible.

- This document may contain data, which exceeds the sheet parameters. It was furnished in this condition by the organizational source and is the best copy available.

- This document may contain tone-on-tone or color graphs, charts and/or pictures, which have been reproduced in black and white.

- This document is paginated as submitted by the original source.

- Portions of this document are not fully legible due to the historical nature of some of the material. However, it is the best reproduction available from the original submission.

COLUMBIA UNIVERSITY

DEPARTMENT OF PHYSICS

■ PROGRESS REPORT No. 18

MAY 1, 1968 THROUGH OCTOBER 31, 1968

To:

THE JOINT SERVICES TECHNICAL ADVISORY COMMITTEE

REPRESENTING: THE U.S. ARMY ELECTRONICS LABORATORIES
THE U.S. ARMY RESEARCH OFFICE
THE OFFICE OF NAVAL RESEARCH
THE AIR FORCE OFFICE OF SCIENTIFIC RESEARCH

COLUMBIA RADIATION LABORATORY NEW YORK, NEW YORK 10027

■ OCTOBER 31, 1968

COLUMBIA RADIATION LABORATORY

RESEARCH INVESTIGATION DIRECTED TOWARD
EXTENDING THE USEFUL RANGE OF THE
ELECTROMAGNETIC SPECTRUM

Progress Report No. 18

May 1, 1968 through October 31, 1968

Contract DA 28-043 AMC-00099(E)
(Continuation of Contract DA 36-039 SC-90789)

CU-10-68 AMC-00099(E) Physics

Object of the research:

Physical research in fields in which microwave frequency tech-
niques are employed; the development of microwave electronic
and circuit devices.

Submitted by: S. R. HARTMANN, Director

Coordinated by: V. M. Bennett, Editor

COLUMBIA UNIVERSITY

Division of Government Aided Research
New York, N. Y. 10027

October 31, 1968

i

Reproduction in whole   or   in part is permitted
for any purpose of the United States Government.

TABLE OF CONTENTS

FACTUAL DATA, CONCLUSIONS, AND PROGRAMS FOR THE NEXT INTERVAL

      The names of the authors are arranged alphabetically.

PUBLICATIONS AND REPORTS

Publications

Michael W. Swagel[1] and Allen Lurio, "g_J Factor of the Lowest $^1P_1$ and $^3P_1$ States of Ba; Level-Crossing Determination of $A(^1P_1)/\mu_0 g_J(^1P_1)$ of Hg^{199}," Phys. Rev. <u>169</u>, 114 (1968).

B. S. Mathur,[2] H. Tang, and W. Happer, "Light Shifts in the Alkali Atoms," Phys. Rev. <u>171</u>, 11 (1968).

W. Happer, "A Partial Wave Expansion of the Finite Rotation Operator," Ann. Phys. (N. Y.) <u>48</u>, 579 (1968).

P. Feldman,[3] M. Levitt, and R. Novick, "Energies and Lifetimes of the Metastable Autoionizing $(1s2s2p)^4 P_J$ States of Li^6 and Li^7; Assignment of Li I^b Quartet Lines," Phys. Rev. Letters <u>21</u>, 331 (1968).

G. Sprott and R. Novick, "Identification of the Metastable Autoionizing States in Potassium with a New Radio-Frequency Spectroscopic Technique," Phys. Rev. Letters <u>21</u>, 336 (1968).

D. Tse and S. R. Hartmann, "Nuclear Spin-Lattice Relaxation Via Paramagnetic Centers without Spin Diffusion," Phys. Rev. Letters <u>21</u>, 511 (1968).

R. E. Miller, W. G. Fastie (Johns Hopkins University), and R. C. Isler,[4] "Rocket Studies of Far-Ultraviolet Radiation in an Aurora," J. Geophys. Res. <u>73</u>, 3353 (1968).

---

1. Present Address: Electro-Optical Systems, 300 North Halsted Street, Pasadena, California 91107.
2. Present Address: Physics Department, Indian Institute of Technology, Kanpur, U. P., India.
3. Present Address: Physics Department, The Johns Hopkins University, Baltimore, Maryland 21218.
4. Present Address: Department of Physics and Astronomy, University of Florida, Gainesville, Florida 32601.

Robert W. Schmieder, Allen Lurio, and W. Happer, "Hyperfine Structure and Lifetimes of the $4^2 P_3/_2$ and $5^2 P_3/_2$ States of K^{39}," Phys. Rev. 173, 76 (1968).

B. S. Mathur,[2] H. Tang, R. Bulos, and W. Happer, "Microwave Light Modulation by an Optically Pumped Rb-87 Vapor," Phys. Rev. Letters 21, 1035 (1968).

Papers by CRL Staff Members Presented at Scientific Meetings

S. R. Hartmann, "Photon, Spin, and Raman Echoes," International Quantum Electronics Conference, Miami, Florida, 14-17 May 1968.

International Atomic Physics Conference, New York, N. Y., 3-7 June 1968.

J. Artura, R. Novick, and N. Tolk, "$He^+(2S)$ Two-Photon Spectrum and the Excitation of Atoms with Metastable He Ions."

S. Dworetsky, R. Novick, W. W. Smith, and N. Tolk, "Inelastic He^+ - He Collisions."

L. M. Blau, R. Novick, and D. Weinflash, "Helium Negative Ion Lifetime."

M. Levitt and R. Novick, "Energies and Lifetimes of the Metastable Autoionizing $(1s2s2p)^4 P_J$ States of Li^6 and Li^7; Assignment of Li I Quartet Lines."

G. F. Sprott and R. Novick, "Magnetic Resonance Spectroscopy of Metastable Autoionizing Atoms."

W. Happer, "Effective Operators in Optical Pumping," International Conference on Optical Pumping and Atomic Line Shape, Warsaw, Poland, 25-28 June 1968 (to be published).

C. J. Artura, R. Novick, and N. Tolk, "$He^+(2S)$ - He Inelastic Collisions," Twenty-First Gaseous Electronics Conference, University of Colorado, Boulder, Colorado, 16-18 October 1968.

Radiation Laboratory Seminars

Meetings are held weekly at Columbia University, New York,
N. Y., during the academic year and are open to all members of
the physics department. Guest speakers are invited to discuss
work in the general area of the research in the Columbia Radia-
tion Laboratory.

C. C. Grimes, Bell Telephone Laboratories, Inc., "Helicon Waves
   in Metals," May 10, 1968.

M. Weisskopf, Brandeis University, "The Electric Dipole Moment
   of the Cesium Atom — An Upper Limit to the Electric
   Dipole Moment of the Electron," May 17, 1968.

R. E. Slusher, Bell Telephone Laboratories, Inc., "Photon
   Echoes in Gases," May 24, 1968.

A. J. DeMaria, United Aircraft Research Laboratories, "Genera-
   tion and Measurement of Picosecond Laser Pulses,"
   October 4, 1968.

K. Prendergast, Astronomy Department, Columbia University, "A
   Model for Certain X-Ray Sources," October 11, 1968.

J. E. Faller, Wesleyan University, "Precision Laser Measure-
   ments: Ranging to the Moon; Interferometric Determina-
   tion of g," October 18, 1968.

P. Thaddeus, Institute for Space Studies, "Detection of Inter-
   stellar C^{13} and Determination of the C^{12}/C^{13} Ratio,"
   October 25, 1968.

Lectures

W. Happer, "Optical Pumping Theory:" a series of lectures
   given at the Summer Institute of Theoretical Physics,
   University of Colorado, Boulder, Colorado, July 1968
   (to be published).

W. W. Smith, "Interference Effects in Ion-Atom Excitation,"
   Seminar, Space Physics Department, Aerospace Corporation,
   El Segundo, California, July 24, 1968.

ABSTRACT

The spectral distribution of the two-photon emission from the metastable $2^2S_{1/2}$ state of singly ionized helium has been verified. Two-photon coincidence counting rates were observed experimentally and agree with those calculated from the theoretically predicted spectral distribution of the two-photon emission. In addition, radiation due to the impact of low-energy metastable singly ionized helium on helium and on the other rare gases has been detected.

An rf resonance experiment has been initiated to make a high precision determination of the fine-structure intervals and the quadrupole coupling constant of the $(1s2s2p)^4P^o$ metastable autoionizing state of lithium. A summary is given of the current status of the experimental work.

The quenching of optically excited atoms by foreign gases can greatly improve the efficiency of optically pumped devices by eliminating the fluorescently scattered light and the concomitant depumping of the atoms. An experimental method which makes use of the optical pumping of alkali vapors is presently being employed in a systematic study of the quenching of excited alkali atoms.

Intensity modulation of light at the 6.835 GHz hyperfine frequency of Rb^{87} has been observed for the first time. In addition to affording possibilities for several practical applications, hfs light modulation experiments are of considerable intrinsic interest since they present one with an ideal system for detailed investigations of parametric frequency conversion in the optical region.

A magnetic rotation spectrum of molecular cesium has been observed for the first time. A partial rotational analysis of the (1,0) band of the 7500-Å band system of Cs_2 gives a value of 0.00104 cm^{-1} for B"-B'. The extrapolated band-head frequency from the rotational analysis and the observed MRS line frequency are in excellent agreement.

A general theory has been developed to account for the echo behavior due to the interactions between the echo atoms and the magnetic nuclei of neighboring atoms. The theory has been applied

to both electron spin and photon echoes in Cr^{3+} doped Al_2O_3 (ruby). A program has also been initiated for studying Raman echoes in scattered light.

A rocket-borne x-ray polarimeter, which makes use of the polarization dependence of Thomson scattering, was successfully flown on July 26, 1968. During this flight, x-ray polarization data were obtained for the bright x-ray source Sco XR-1 of the constellation Scorpio. In addition, a new x-ray telescope is being constructed to study the soft x-ray stars in the 44-100 Å region of the spectrum.

I. ATOMIC PHYSICS

A. METASTABLE ATOMS AND IONS

1. Properties of the Metastable State of Singly Ionized Helium

a. Direct Detection of the Two-Photon Decay Mode[*]
(C. J. Artura, R. Novick, N. Tolk)

In order to study the spectral distribution of the decay photons, we have replaced one of the "hard" uv phototubes with a "soft" uv phototube. While keeping the system in operation, we are able to place various broadband filters over the face of the "soft" uv phototube. These filters, which include MgF_2, CaF_2, SrF_2, BaF_2, Al_2O_3, and Suprasil (fused silica), have various low-wavelength cutoff limits and transmission characteristics. The coincidence counting rates with the various filters give us information about the two-photon spectral distribution. Table I presents the data obtained.

In Table I, S/S_o is the ratio of the single-photon counting rate with a specific filter to that with no filter; R/R_o is the ratio of the coincidence counting rate with a specific filter to that with no filter. Columns 3 and 4 give the experimental values for singles and coincidences with their corresponding uncertainties. Columns 5 and 6 give the singles and coincidence values computed from the theoretical expressions

$$\frac{S}{S_o} = \frac{\int_{\nu_1}^{\nu_3} T(\nu)\eta(\nu)A(\nu)\,d\nu}{\int_{\nu_1}^{\nu_2} \eta(\nu)A(\nu)\,d\nu} \quad ,$$

and

$$\frac{R}{R_o} = \frac{\int_{\nu_1}^{\nu_3} T(\nu)\eta(\nu)\eta'(\nu_o-\nu)A(\nu)\,d\nu}{\int_{\nu_1}^{\nu_2} \eta(\nu)\eta'(\nu_o-\nu)A(\nu)\,d\nu} \quad ,$$

TABLE I. Comparison of Experimental and Theoretical Results
on Two-Photon Spectrum.

Relative Singles and Coincidence Rates with Filters

Filter	Cutoff	S/S_o Experimental	R/R_o Experimental	S/S_o Theoretical	R/R_o Theoretical
MgF_2	1130 Å	0.7128 ± 0.0051	0.63 ± 0.15	0.697	0.696
CaF_2	1225 Å	0.6633 ± 0.0049	0.50 ± 0.15	0.570	0.569
SrF_2	1275 Å	0.6451 ± 0.0051	0.61 ± 0.16	0.529	0.528
BaF_2	1325 Å	0.6709 ± 0.0049	0.48 ± 0.14	0.5045	0.5046
Al_2O_3	1425 Å	0.5334 ± 0.0044	0.46 ± 0.12	0.491	0.493
Suprasil	1600 Å	0.4749 ± 0.0042	0.32 ± 0.12	0.423	0.419

$$\frac{S}{S_o} = \frac{\int_{\nu_1}^{\nu_3} T(\nu)\eta(\nu)A(\nu)\,d\nu}{\int_{\nu_1}^{\nu_2} \eta(\nu)A(\nu)\,d\nu}$$

$$\frac{R}{R_o} = \frac{\int_{\nu_1}^{\nu_3} T(\nu)\eta(\nu)\eta'(\nu_o-\nu)A(\nu)\,d\nu}{\int_{\nu_1}^{\nu_2} \eta(\nu)\eta'(\nu_o-\nu)A(\nu)\,d\nu}$$

ν_1 (3500 Å) , ν_2 (1050 Å) , ν_3 (Filter Cutoff)

4

where ν_1 and ν_2 are the frequencies corresponding to the wavelengths of 3500 Å and 1050 Å, respectively, and ν_3 is the frequency corresponding to the low-wavelength cutoff limit of the specific filter. $T(\nu)$ is the transmission of the filter, $A(\nu)$ is the two-photon spectral distribution, η is the efficiency of the "soft" tube, and η' is the efficiency of the "hard" tube. The transmission characteristics of our filters were measured to within 5% by Dr. J. A. R. Samson of the GCA Corporation. A paper by Samson and Cairns[1] provided information on the approximate efficiency of the "hard" tube; information on the efficiency of the "soft" tube was provided by the manufacturer. For the two-photon spectral distribution, we used the carefully calculated values of Spitzer and Greenstein.[2]

We have chosen to present the comparison between experimental and theoretical results in terms of the ratios of counting rates rather than in terms of absolute counting rates. The calculation of the latter would require the use of frequency-independent as well as frequency-dependent quantities. Some of these frequency-independent quantities are complicated and difficult to calculate; furthermore, some are not very well known. However, when we deal with the ratios of counting rates, these troublesome frequency-independent quantities cancel out, thus removing one cause of uncertainty from our theoretical results. Furthermore, the phototube efficiencies used in the calculation could differ from the actual efficiencies by a factor of proportionality without affecting the calculated ratios of counting rates; however, this would cause an error in the calculated absolute counting rates. In other words, the former calculation requires only relative phototube efficiencies, while the latter requires absolute phototube efficiencies. Besides, uncertainties in the phototube efficiencies would affect the former calculation less seriously than the latter calculation. In

view of these considerations, the relative counting rates provide a better test of the theoretical two-photon spectral distribution than the absolute counting rates.

Table I shows that the theoretical relative coincidence counting rates agree with the experimental relative coincidence counting rates. On the other hand, the singles counting rates show no such agreement. But we should not expect to find agreement in this case. The two-photon emission is the only source of true coincidences resulting from the metastable component of the beam. However, it is not the only source of a singles counting rate resulting from the metastable component of the beam. Another source is the radiation due to the impact of metastable ions on the background gas. Thus the coincidences provide the only true test of the spectral distribution of the double-photon decay spectrum of metastable He^+. Therefore, the agreement between the theoretical and experimental values of the relative coincidence rates serves as a verification of the theoretical two-photon spectral distribution.

In order to test the sensitivity of our experiment to the spectral distribution of the two-photon emission, we calculated S/S_O and R/R_O using three other spectral distribution functions $A(\nu)$. The simplest test spectrum to consider is a uniform spectral distribution. This distribution, denoted as $A_{flat}(\nu)$, is independent of frequency and has the form $A_{flat}(\nu) \propto 1$ for $0 \leq \nu \leq \nu_O$. The second test spectrum, $A_{NU3}(\nu)$, is defined as proportional to the cube of the product of the frequencies of the two photons, i.e., $A_{NU3}(\nu) \propto \nu^3(\nu_O-\nu)^3$. Such a distribution results from considering only the phase space factor in the theoretically predicted two-photon spectral distribution, $A_{normal}(\nu)$, and neglecting the matrix element factor. The final test spectrum to be considered, the reverse spectrum, is obtained by reflecting the theoretically predicted spectrum about $\nu_O/4$ for $0 \leq \nu \leq \nu_O/2$ and about $3\nu_O/4$ for $\nu_O/2 \leq \nu \leq \nu_O$. Therefore, $A_{reverse}(\nu) =$

$A_{normal}[(\nu_o/2)-\nu]$ for $0 \leq \nu \leq \nu_o/2$, where $A_{normal}(\nu)$ is the
theoretically predicted spectrum tabulated by Spitzer and
Greenstein. The results of these calculations are presented in
Table II. The values of R/R_o calculated with these various spec-
tral distributions fall within the uncertainties of the experi-
mental values except for Suprasil in the case of the flat spec-
trum, strontium fluoride and calcium fluoride in the case of the
NU3 spectrum, and Suprasil in the case of the reverse spectrum.
Only the values calculated using the normal spectrum agree with
the experimental values in all cases. This fact and further
comparison of experimental and calculated values in Table II
show that the values calculated from the theoretically predicted
(normal) spectrum provide the best agreement with the experi-
mental data.

We have mentioned that in the two-photon decay one photon
has a wavelength lying between 304 Å and 608 Å, and the comple-
mentary photon has a wavelength greater than 608 Å. This is due
only to conservation of energy. Since the "soft" phototube is
sensitive from 1050 Å to 3500 Å, two such "soft" phototubes can-
not detect a two-photon coincidence. To verify that indeed there
are no "soft"-"soft" coincidences, we set two "soft" phototubes
at an angular separation of 120° and look for coincidences be-
tween these two tubes. Since cosmic rays produce a troublesome
coincidence background, we surround each phototube with a con-
centric cylindrical shell of plastic scintillator which acts as
an anticoincidence shield against cosmic rays. "Soft"-"soft"
coincidences are accepted but "soft"-"soft"-scintillator triple
coincidences are rejected, thereby eliminating the coincidences
due to cosmic rays. In this way, we eliminate at least 70% of
the cosmic-ray coincidence background.

We are prevented from observing a truly null signal
because of statistical fluctuations in the chance coincidence
background, i.e., the beam-dependent coincidences due to

TABLE II. Sensitivity of Experimental Results to Various Spectral Distributions.

EMI-EMR Relative Coincidence Rates with Filters

Filter	R/R_o Experimental	R/R_o Normal	R/R_o Flat	R/R_o $\nu^3(\nu_o-\nu)^3$	R/R_o Reverse
MgF_2	0.63 ± 0.15	0.696	0.718	0.608	0.726
CaF_2	0.60 ± 0.15	0.569	0.600	0.448*	0.611
SrF_2	0.61 ± 0.16	0.528	0.561	0.400*	0.572
BaF_2	0.48 ± 0.14	0.5046	0.543	0.358	0.555
Al_2O_3	0.46 ± 0.12	0.493	0.529	0.348	0.541
Suprasil	0.32 ± 0.12	0.419	0.466*	0.253	0.480*

* indicates lack of agreement between experimental and calculated values.

uncorrelated events. Therefore, we can only set an upper limit to the occurrence of a "soft"-"soft" coincidence. This upper limit decreases as $t^{-\frac{1}{2}}$, where t is the running time; we can make this upper limit as small as we like by accumulating data for a sufficiently long time. However, since $t^{-\frac{1}{2}}$ approaches its asymptotic value of zero slower and slower as t increases, we soon reach a point of diminishing returns. By collecting data for 56 hours, we are able to establish an upper limit of 0.098 counts per minute, i.e., "soft"-"soft" coincidence rate $\lesssim$ 0.098 counts per minute. To get some idea of the smallness of this quantity, we compare it with the "hard"-"soft" coincidence rate, which is typically 6 counts per minute. Thus we have shown that the "soft"-"soft" coincidence rate is at least a factor of 60 smaller than the "hard"-"soft" rate and that our observations are consistent with the theoretical prediction of a zero rate for this quantity.

In summary, we have verified the spectral distribution of the two-photon emission from the metastable $2^2S_{1/2}$ state of singly ionized helium. We observed the two-photon coincidence counting rates with a "hard" uv phototube and a "soft" uv phototube over whose face we were able to place various broadband filters. These experimental coincidence counting rates agree with the coincidence counting rates calculated from the theoretically predicted spectral distribution of the two-photon emission, but we have not been able to provide a critical test of the theory in the sense that other spectral distributions are also consistent with our observations. However, we have certainly shown that the coincidence spectrum is continuous. We have also shown that the theoretically null "soft"-"soft" coincidence counting rate is less than 1/60 of the "hard"-"soft" coincidence counting rate. This residual coincidence counting rate is due only to statistical fluctuations in the chance coincidence background. Furthermore, we have detected radiation due to the

impact of low-energy metastable singly ionized helium on helium and on the other rare gases.

Program for the next interval: We shall resume work on the lifetime of metastable He^+.

(1) R. B. Cairns and J. A. R. Samson, GCA Technical Report No. 66-17-N, pp. 10-12.

(2) L. Spitzer and J. L. Greenstein, Astrophys. J. <u>114</u>, 407 (1951).

---

2. Metastable Autoionizing Atoms

a. Rf Spectroscopy of Metastable Alkali Atoms
(R. Novick, G. Sprott)

The magnetic resonance apparatus has been changed somewhat to allow for future installation of components which would improve the versatility of the anticipated measurements. The main change has been to move the A magnet from the source chamber to the detector chamber. With this alteration, it will be possible to reinstall an electron gun of the design originally used by Feldman.[1] His design was not used for the resonance experiments because it was felt that the electron beam produced would be severely attenuated by the fringing field of the A magnet. However, the present electron gun yields electron fluxes significantly smaller than the earlier design, and this makes it important that we try to reincorporate Feldman's electron gun in the present apparatus. A second modification involves the installation of a $7\frac{1}{2}$ in. extension to the detector chamber. This would give us enough room to install a metastable atom detector which is movable along the beam axis. With such a movable detector, it should be possible to measure the lifetimes of the individual metastable states in potassium.

The modified apparatus has been tested, and measurements of the metastable rubidium atom are under way. The technique used is the same as that reported in reference 2 except that the A and B magnets have inhomogeneous fields. This allows calibration of the C magnets from Zeeman transitions in the rubidium ground state. Preliminary results indicate that the metastable autoionizing state of Rb is a $(4p^5 5s5p)^4D_{7/2}$ state.

In addition to the new series of experimental measurements, we are continuing to study the results obtained for potassium. Two recent developments have encouraged further study of the metastable potassium atom. First, we were informed that W. R. S. Garton and M. Mansfield of Imperial College in London have measured the optical KI[b] absorption spectrum of potassium, and it is likely that their spectra include several lines terminating on states of the $(3p^5 4s3d)$ configuration, which contains one of the observed metastable autoionizing states. From the position of these lines, which had not previously been observed, we might be able to ascertain the strengths of coupling between the electrons in this configuration. Secondly, Hartree-Fock calculations of the wave functions and Slater parameters for the $(3p^5 4s3d)$ and $(3p^5 4s4p)$ configurations were recently undertaken by W. Martin and M. Wilson at the National Bureau of Standards in Washington, D. C., and they have supplied us with their results. Since our analysis of the potassium spectrum is not yet complete, we do not give the details in this report. It will suffice to say that we will use the data given us by Martin and Wilson to obtain a reasonable estimate of the level structure of the $(3p^5 4s3d)$ configuration, and we hope to be able to achieve a fit between these theoretical estimates and the experimental data of Garton.

In a previous Progress Report,[3] we gave an argument for our conclusion that the observed $^4D_{7/2}$ state in potassium belongs to the $(3p^5 4s4p)$ configuration rather than to the $(3p^5 4s3d)$.

This argument rested on the fact that the quadrupole coupling constant should be of equal but of opposite sign for the $(3p^54s3d)^4D_{7/2}$ and $(3p^54s4p)^4D_{7/2}$ states. Since the experimental value of B agreed in sign with that predicted for the $(3p^54s4p)^4D_{7/2}$ state, we concluded that the observed metastable state was from the $(3p^54s4p)$ configuration. It was assumed at the time that both states under consideration were eigenstates of $\vec{L}$ and $\vec{S}$. However, the $(3p^54s3d)^4D_{7/2}$ state is most probably not a pure state but is mixed with other states with $J = 7/2$ in the same configuration, and conceivably this mixing might be sufficient to change the sign that we would predict for B. The major restraint on the amount of mixing is that the measured g_J value of the metastable $^4D_{7/2}$ state would be expected to differ from the projected Russell-Saunders value if appreciable mixing occurred. We derive below a mathematical expression for the range of values that B may assume in the $(3p^54s3d)^4D_{7/2}$ state subject to the constraint provided by the experimentally determined g_J value.

Any $J = 7/2$ state of the $(3p^54s3d)$ configuration can be expanded in terms of eigenstates of $\vec{L}$ and $\vec{S}$ in the following way.

$$
\begin{aligned}
|\psi_{7/2}\rangle \;=\; & b_1 |(3p^54s)^3P, 3d, {}^4D_{7/2}\rangle \\
& + b_2 |(3p^54s)^3P, 3d, {}^4F_{7/2}\rangle \\
& + b_3 |(3p^54s)^3P, 3d, {}^2F_{7/2}\rangle \\
& + b_4 |(3p^54s)^1P, 3d, {}^2F_{7/2}\rangle \quad , \qquad (1)
\end{aligned}
$$

where the parent L-S eigenstates are shown explicitly. Since the expansion coefficients must satisfy the condition

$$
\sum_i |b_i|^2 \;=\; 1 \quad , \qquad (2)
$$

we can make the following substitutions:

$$b_1 \equiv Ae^{i\theta} \quad , \quad \text{where } A > 0 \quad ,$$

$$b_2 \equiv e^{i\varphi}[1-A^2 - (|b_3|^2 + |b_4|^2)]^{\frac{1}{2}} \quad , \tag{3}$$

where φ and θ are the phases of the complex numbers b_1 and b_2. The quadrupole coupling constant and g_J for the mixed $J = 7/2$ state are given, in terms of the expansion coefficients, by:

$$B = b'_{3p}\left[|b_1|^2 - \tfrac{2}{3}|b_2|^2 - (|b_3|^2 + |b_4|^2) - \tfrac{4}{\sqrt{6}}\, Re(b_1 b_2)\right] \tag{4}$$

and

$$g_J = -1.4296|b_1|^2 - 1.2386|b_2|^2$$

$$-1.1432(|b_3|^2 + |b_4|^2) \quad , \tag{5}$$

where the quadrupole interaction with the 3d electron has been assumed negligible,[4] and the g_J values for the L-S eigenstates in Eq. (1) are given explicitly. The single-electron coupling constant b'_{3p} is defined by $b'_{3p} = \tfrac{2}{5}\, e^2 Q\langle r^{-3}\rangle_{3p}$. In terms of the constants defined in (3), we obtain

$$B = b'_{3p}\left[-\tfrac{2}{3} + \tfrac{5}{3}A^2 - \tfrac{1}{3}(|b_3|^2 + |b_4|^2)\right.$$

$$\left. - \tfrac{4A}{\sqrt{6}}\left(1-A^2-(|b_3|^2 + |b_4|^2)\right)^{\frac{1}{2}}\cos(\varphi - \theta)\right] \quad , \tag{6}$$

and

$$g_J = -1.2386 - A^2(0.1910) + 0.0954(|b_3|^2 + |b_4|^2) \quad . \tag{7}$$

From the experimental value of g_J, i.e., $g_J = 1.42945 \pm 0.0002$, we can state that $g_J \geq 1.4292$. This requires that

$$A^2 \geq 0.9979 \pm 0.05(|b_3|^2 + |b_4|^2)$$

$$\tag{8}$$

or

$$A \geq 0.999 \quad .$$

13

If we apply (2), we also obtain

$$|b_3|^2 + |b_4|^2 \leq 0.0021 \quad . \tag{9}$$

Finally, by substituting (8) and (9) into (6), we find that

$$B \geq +0.996 \ b'_{3p} \quad . \tag{10}$$

Thus, the amount of mixing allowed by the experimental value of g_J is not sufficient to change B by more than 1%, let alone change its sign, to make it agree with the negative value observed experimentally (in ref. 3, b'_{3p} was shown to be positive). This validates our previous argument.

The above conclusion is also in agreement with the results obtained by Martin and Wilson for the $(3p^5 4s3d)$ configuration. Using the Slater coefficient from the output of their Hartree-Fock program, they diagonalized the combined spin-orbit and electrostatic interaction matrix to obtain the expansion coefficient of Eq. (1). Their results give a 7% admixture of one of the short-lived $^2F_{7/2}$ states with the $^4D_{7/2}$ state. Not only would the lifetime of this impure $^4D_{7/2}$ state be too short to have been observed in our atomic beam experiment, but the value of g_J calculated for the state ($g_J = -1.407$) disagrees with our measured value for the $^4D_{7/2}$ state.

(1) CRL Quarterly Progress Report, December 15, 1962, p. 11.

(2) CRL Progress Report, April 30, 1966, p. 4.

(3) CRL Progress Report, October 31, 1967, p. 7.

(4) This assumption has been substantiated by a recent Hartree-Fock calculation.

---

b. Zeeman Quenching[*]
   (M. R. Levitt, R. Novick, S. Skwire)

In the last Progress Report[1] we summarized and interpreted the experimental results derived from an atomic-beam

14

Zeeman-quenching experiment on the $(1s2s2p)^4P^o$ metastable auto-ionizing state of Li.[2] We also indicated that the determination of the energies (to an accuracy of 100-300 ppm) and lifetimes (to an accuracy of about 50%) of the $^4P^o$ fine and hyperfine levels could serve as the basis for more precise measurements by use of rf resonance techniques. We now describe this program in somewhat greater detail.

In an earlier report,[3] we identified the three pairs of differentially metastable levels of Li^7 for which two states interact over localized magnetic field regions, thereby giving rise to observable anticrossing signals. It was found that for Li^7, the states of interest, as specified by the quantum numbers appropriate at low field, are $|J = 1/2, F = 2\rangle$, $|J = 1/2, F = 1\rangle$, $|J = 5/2, F = 4\rangle$, and $|J = 5/2, F = 3\rangle$. A plot of energy vs field for most of the magnetic sublevels of these states is shown in Fig. 1. It can be seen that in addition to the three anticrossings, there are a number of fields at which states having different magnetic quantum numbers cross. Of special interest are those pairs of crossing levels whose wave functions (and hence, lifetimes) are similar to the respective members of an anticrossing pair. If it is possible to produce strong coupling of these states with an rf magnetic field, one can then effect a change in metastable beam strength which is comparable to that of the anticrossing case. As an alternative to the point of view that a photon is created or annihilated in conjunction with the transition of an atom from a long-lived to a short-lived state, one can adopt the view that in a reference frame rotating with the angular frequency of the applied rf field, the two levels anticross. The difference between the case of anticrossing in a static field as opposed to "anticrossing" in an rf field is that in the latter case the linewidth is limited only by the natural width of the short-lived state since one can continuously vary the size of the interaction which couples the two levels.
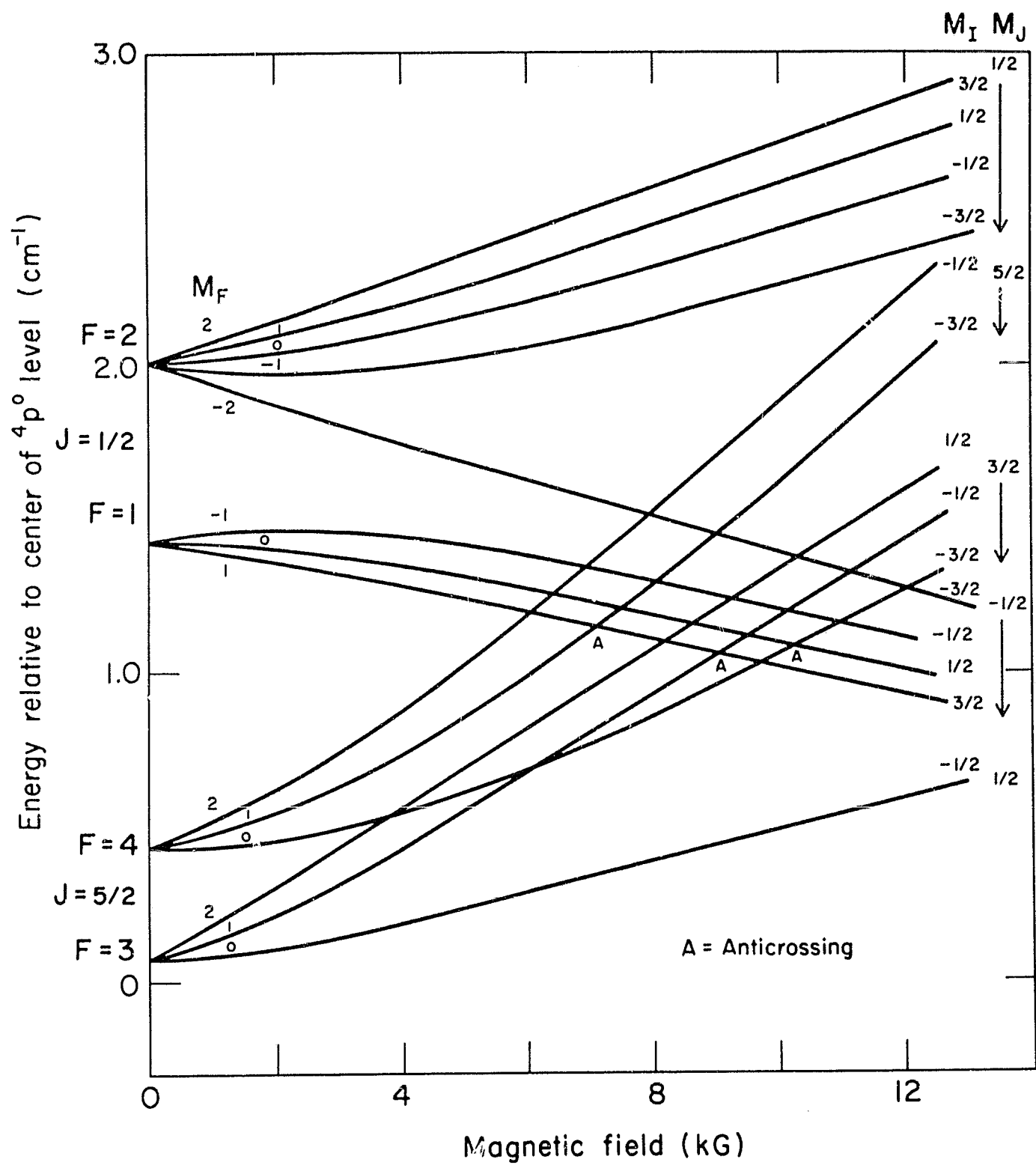
15

FIG. 1. Plot of energy vs magnetic field for various $(1s2s2p)^4p^O$ substates.

The two levels associated with the largest anticrossing signal are shown as solid lines in Fig. 2a. The variation of the state lifetimes with magnetic field is shown in Fig. 2b, which also clearly indicates why a symmetric dip in metastable beam strength is observed experimentally. In addition, the figure shows the energy and lifetime behavior of a third level which is short lived and becomes degenerate in energy with the long-lived member of the anticrossing pair at a field value below the anti-crossing point. On the basis of our previous discussion, the crossing levels are appropriate selections for resonance studies if suitable rf coupling can be provided. It can be shown that the rate of stimulated magnetic dipole transitions from the long-lived to the short-lived state is given by

$$W = \frac{\frac{1}{4} \gamma_{SL} |V|^2}{(\nu-\omega)^2 + \frac{1}{4} \gamma_{SL}^2} \quad \text{sec}^{-1} \quad , \qquad (1)$$

and the first-order expression for the resonance signal is[4]

$$S = C \frac{|V|^2}{4(\nu-\omega)^2 + \gamma_{SL}^2 + (\gamma_{SL}/\gamma_{LL})|V|^2} \quad . \qquad (2)$$

In expressions (1) and (2), γ_{SL} and γ_{LL} are the decay rates of the short-lived and long-lived states, respectively; $\hbar\nu$ is the energy separation of the two states; ω is the circular frequency of the applied rf field; and $\hbar V$ is the matrix element of the interaction energy between atom and rf field. In Fig. 2c, we plot S as a function of magnetic field for various values of the rf magnetic field amplitude.

A small extension of the previous remarks is required to complete the plan for the proposed atomic-beam resonance experiment. Imagine that the long- and short-lived states of interest are produced by electron bombardment of neutral ground-state atoms. If the atoms travel only 0.1 cm before entering a region
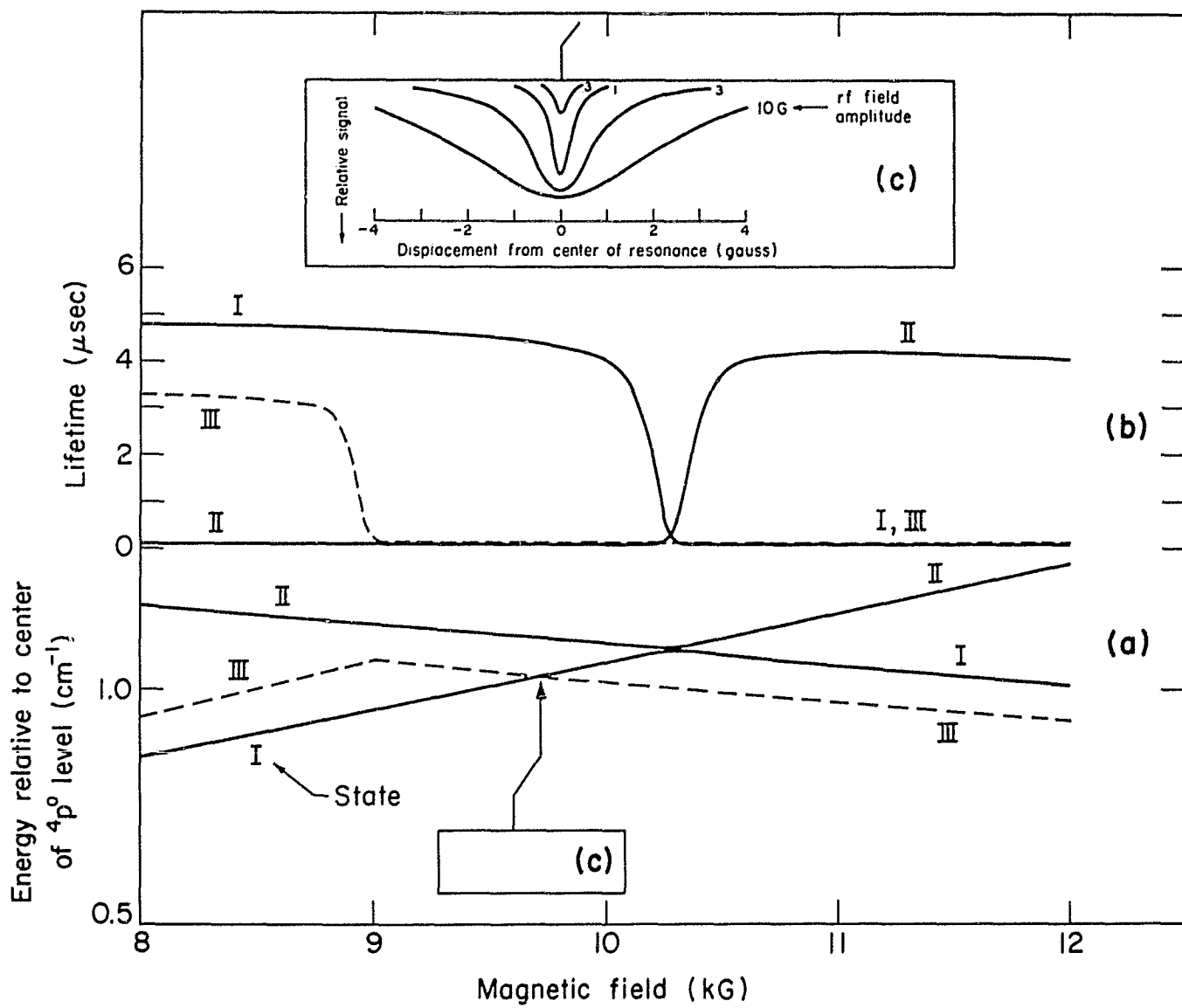
FIG. 2. a) Plot of energy vs magnetic field for three
differentially metastable states. b) Plot of
lifetime vs magnetic field for three differen-
tially metastable states. c) Theoretical
resonance signal as a function of uniform mag-
netic field for various rf magnetic field
amplitudes.

18

containing an rf field, practically all of the short-lived atoms will have decayed (about one in 10^4 survive), while most of the long-lived atoms have not autoionized. The rf field will then have a beam-quenching effect since transitions will be induced preferentially to the short-lived level. The differential meta-stability of the two states in question thus serves as a state-selecting mechanism before the rf region and as a state-analyzing mechanism afterward.

In practice, the rf transition fields are produced in a loop which consists of a length of coaxial waveguide which is shorted at one end. The coaxial cable which is used as the rf transmission line is chosen to be about one fourth as long as the rf wavelength, so that the impedance of the line and loop is purely resistive for 30-MHz propagation. An rf magnetic field antinode is therefore obtained at the shorted end of the loop through which the beam passes. Using a tuned Millen rf amplifier as the last stage of the rf generation and amplification system, we have produced rf fields of the order of 1 G in the region of beam traversal, which is almost sufficient for resonance satura-tion.

The experimental determination of the energy splitting as a function of magnetic field for two crossing levels must be re-lated to the Zeeman Hamiltonian for the $^4P^o$ state in order to extract the fine- and hyperfine-structure interaction constants. We will not go into the details of this problem here except to indicate the form of the appropriate first-order energy terms and associated correction terms. The first-order Hamiltonian for the $^4P^o$ state can be written in the form[5]

$$\mathcal{K} = c_{SO}\,\vec{L}\cdot\vec{S} + c_{SS}[(3/2)(\vec{L}\cdot\vec{S}) + 3(\vec{L}\cdot\vec{S})^2 - L(L+1)S(S+1)] + a_c\,\vec{I}\cdot\vec{S}$$

$$+ c_{MD}\{\vec{I}\cdot\vec{L} + \frac{1}{S(2L-1)(2L+3)}[(\vec{I}\cdot\vec{S})L(L+1) - \frac{3}{2}(\vec{I}\cdot\vec{L})(\vec{L}\cdot\vec{S}) - \frac{3}{2}(\vec{L}\cdot\vec{S})(\vec{I}\cdot\vec{L})]\}$$

$$+ c_Q\frac{[3(\vec{I}\cdot\vec{J})^2 + \frac{3}{2}(\vec{I}\cdot\vec{J}) - I(I+1)J(J+1)]}{2I(2I-1)J(2J-1)}\,f_J + (g_L L_Z + g_S S_Z - g'_I I_Z)\mu_o H\,,$$

$$(3)$$

where the interaction constants are as follows: c_{SO}: fine-structure spin-orbit; c_{SS}: fs spin-spin; a_c: hyperfine Fermi contact; c_{MD}: hyperfine magnetic dipole; c_Q: hyperfine electric quadrupole. Manson[5] has estimated that $c_{MD}(Li^7) \approx 0.002$ cm^{-1}, $c_Q(Li^7) \approx 10^{-4}$ cm^{-1}. A precision determination of the quadrupole coupling constant therefore requires taking into account the motional correction to the Zeeman effect ($g_L \to g'_L$) since we have estimated that it causes a shift in energy of order 10^{-5} cm^{-1}. A determination of the fine structure to better than one ppm requires consideration of the relativistic corrections to the Zeeman effect, the higher-order nuclear moments, and the breakdown in L-S coupling. The latter effect has been estimated to contribute shifts to the quartet Zeeman energies of order 10^{-7} cm^{-1}.

Our experimental work has so far consisted of several searches over the magnetic field region of interest for the resonance transitions described earlier. The experimental technique involved setting the electron bombardment voltage several eV above the metastable threshold, applying 100% amplitude modulation to the rf, and using a phase-sensitive lock-in detector to measure changes in the autoionization current. Since we were unable to discern any resonance features during single, slow sweeps over the appropriate range of magnetic fields, we subsequently used a digital signal averager, which stored the lock-in detector output signals from a number of successive sweeps. However, resonance signals have still not been observed. This appears to be related to the fact that the stability of the

20

field over the data-acquisition time period has been about one part in 10^4. This means that the amplitude of a resonance signal of width 0.25 G would be reduced by a factor of about 4, so that sixteen times as many sweeps are required relative to the case of perfect field stability to obtain a given signal strength. We are presently working to improve the stability by a factor of 10, by either manually or electronically compensating for drifts. The search for resonance signals will then be resumed.

(1)   CRL Progress Report, April 30, 1968, p. 11.

(2)   P. Feldman, M. Levitt, and R. Novick, Phys. Rev. Letters 21, 331 (1968).

(3)   CRL Progress Report, October 31, 1967, p. 9.

(4)   W. E. Lamb, Jr. and T. M. Sanders, Jr., Phys. Rev. 119, 1901 (1960).

(5)   S. T. Manson, "The Theory of Autoionization," Ph.D. Thesis, Columbia University, 1966 (unpublished).

---

c. He⁻ Ion
   (L. M. Blau, R. Novick, D. Weinflash)

A number of modifications have been made to improve the performance of the experimental equipment used to study the He⁻ ion beam. A cable-and-spool driving mechanism for positioning the detector assembly was substituted for the screw drive, which caused trouble by damaging the internal signal cable. Added protection was given to the signal cable by increasing the individual wire sizes and twisting in a strength member. The new drive controls the positioning of the detector to ±0.100 in. instead of the previous value of ±0.010 in., but the coarser adjustment will have an insignificant effect on the over-all determination of the component lifetimes.

The front of the detector assembly was modified by the addition of an OFHC copper grid with 93% transmission. The grid will serve to prevent leakage down the tube from the electrostatic

fields on the detector suppressor and, in general, will define
the regions over which electrostatic fields are applied.

Various additional changes have been made on the external
experimental equipment to improve the reliability of operation.

Measurements are now being made on the He^+ beam to deter-
mine the exact effects of the modifications. A new power supply
for the magnet is being installed to allow magnetic fields of
about 1.5 kG in the solenoid to be reached.

Program for the next interval: To resume the investiga-
tion on the He^- ion beam and to improve the determination of the
component lifetimes as a function of magnetic fields by more
precise measurements of the beam energies and applied magnetic
field.

B. LEVEL-CROSSING AND OPTICAL DOUBLE-RESONANCE SPECTROSCOPY

1. Lifetimes and Stark Effect of Excited Atomic States
   (W. Happer, A. Lurio, R. Schmieder)

Because of a change in personnel, this program has been
temporarily interrupted.

---

2. Fine Structure of Singly Ionized Lithium
   (A. W. Adler, T. Lucatorto, R. Novick)

We have continued our effort to measure the 2^3P_J, F = 2 →
F = 1 hfs energy separations in Li_6^+ by an rf magnetic resonance
method. In our previous work we had employed as the source of
the microwave field an adjustable rectangular cavity with a
sliding joint. While this cavity conveniently provided external
adjustment of the resonant frequency, the fringing fields in the
region of the sliding joint created a breakdown of the residual
gas in the cavity. This breakdown effect has been eliminated by
installing a new fixed-frequency cavity and by reducing the

22

residual gas pressure through improved oven shielding and the installation of cooling baffles.

Data taken with the new cavity have indicated the possible presence of a resonance near the predicted region. However, the signal-to-noise ratio was no better than the best of the previous results, and a definite identification of the line still cannot be made. Calculations based on our observation of resonances between the Zeeman levels[1] suggest that the expected signal-to-noise ratio should be about five times that observed. We attribute the increase in noise to a small, unstable microwave power modulation of the light emitted from the lithium beam. Although our present scheme of data averaging[1] compensates somewhat for this effect, the low-frequency components of this unstable source of spurious signal have not been totally eliminated.

Program for the next interval: 1) In order to eliminate the spurious signals generated by the interaction of the microwave field and the lithium beam, two new methods of signal modulation will be tested. One will involve the simultaneous modulation of the detected polarization and the microwave power, and the other the simultaneous modulation of the detected polarization and magnetic field. 2) The strength of the signal will be increased by the use of a new "Super S-11" phototube whose quantum efficiency is 60% higher at $\lambda = 5485$ Å than the currently used S-11 tube. The use of a Lavalle nozzle to increase the lithium beam density is also being investigated.

(1) CRL Progress Report, October 31, 1966, p. 19.

C. COLLISION PHENOMENA

1. Optical Excitation with Low-Energy Ions*
   (S. Dworetsky, R. Novick)

Our investigation of low-energy collision phenomena[1] has continued during this period. Previous work[2] had established the fact that low-energy He^+ ions, when colliding with ground-

state He atoms, were surprisingly efficient in producing excited He atoms. Observation of the resultant photons showed a strongly oscillatory dependence on bombarding energy. Theoretical work in progress seems to indicate that these phenomena are due to a complex electronic interaction hitherto unanticipated. Specifically, the potential curves representing the energy values of the various states of the He^+ - He molecular system exhibit a number of pseudocrossings. Calculations seem to indicate that these pseudocrossings are responsible for our experimental results. This theoretical work has stimulated an experimental search for light resulting from the 2^1P - 1^1S transition (584 Å). A significant motivating factor is the relative ease with which the theoreticians can handle this problem as compared with excitation of higher states.

We have consequently embarked on a program to observe the 584-Å transition. Formidable difficulties have been anticipated in our attempt to observe this radiation. Since this transition is a resonant one (connects the ground state with an excited state) and since the target atoms are all in the ground state, the probability is very great that an emitted 584-Å photon will be reabsorbed by the target He atoms. If the detection system is cylindrical, the process of absorption and re-emission will "transport" the resonant photons to the walls of the system before they can reach the detector.

A second and perhaps more formidable difficulty is due to the relative positions of the 2^1S and 2^1P states of He. The 2^1P state lies above the 2^1S state, and when a resonant photon is reabsorbed, there is a finite probability that it will be emitted as 2-μ light (2^1P - 2^1S transition) and will be lost to our 584-Å detector. Calculations of this trapping effect show it to be a considerable one.

A third difficulty which we are forced to accept is the lack of a filter for 584-Å light. Instead of a filter, we must,

24

therefore, use a grating spectrometer. Its large f number and low-efficiency grating reduce the signal considerably.

A number of experimental setups were considered and tried. The most successful one is illustrated in Fig. 3. We have employed the following improvements to handle the aforementioned difficulties.

(1) The target chamber was terminated with a collodion film backed on 80%-transparency copper mesh 1 cm from the beam. This allows the passage of 584-$\mathring{A}$ radiation and yet holds back the He gas in the target chamber. The small distance of high-pressure He through which the 584-$\mathring{A}$ light has to consequently travel minimizes the trapping and absorption problem.

(2) The differential pumping chamber minimizes the effect of pinholes in the film by maintaining a low pressure of any He which might escape the target chamber.

(3) A McPherson Model 225 normal-incidence 1-meter vacuum uv spectrometer was purchased to provide selection of 584-$\mathring{A}$ radiation.

(4) The grating is platinum coated to maximize its reflectance at 584 $\mathring{A}$.

(5) A low-noise E.M.I. 9603 open-face particle multiplier was used as a detector.

Because of the uncertainty in the efficiencies of the collodion film and grating, as well as the difficulty of making an exact calculation of the trapping effect, only an order-of-magnitude estimate can be made of the expected signal. On this basis we expect a signal of approximately 5-10 counts/sec. No signal was observed with a beam of ground-state He^+ atoms. However, by increasing the electron-bombardment voltage in the He^+ source, we may obtain a larger beam. It should be noted that this beam now contains metastable He^+ as well as He^+ in the ground state. In this mode a signal was observed.
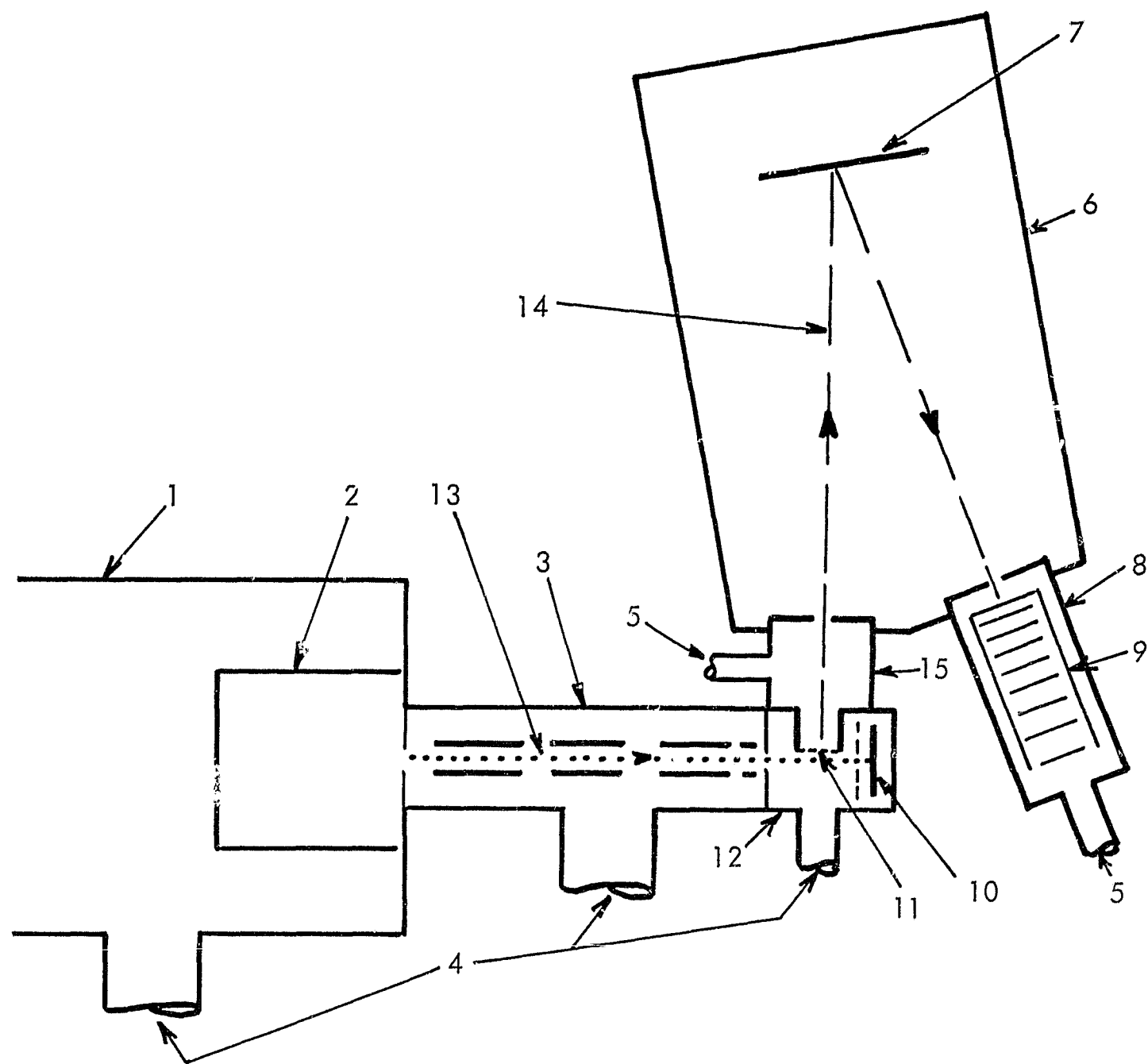
25

FIG. 3. Experimental apparatus for detection of 584-Å
radiation in low-energy He^+- He collisions.

1) Source chamber; 2) He^+ source; 3) intermediate
pumping chamber with differential pumping slits and
electrostatic ion lenses; 4) mercury diffusion
pumps; 5) oil diffusion pumps; 6) spectrometer;
7) grating; 8) detector vacuum chamber; 9) photo-
multiplier; 10) beam detector; 11) collodion film;
12) target chamber; 13) He^+ beam; 14) path of
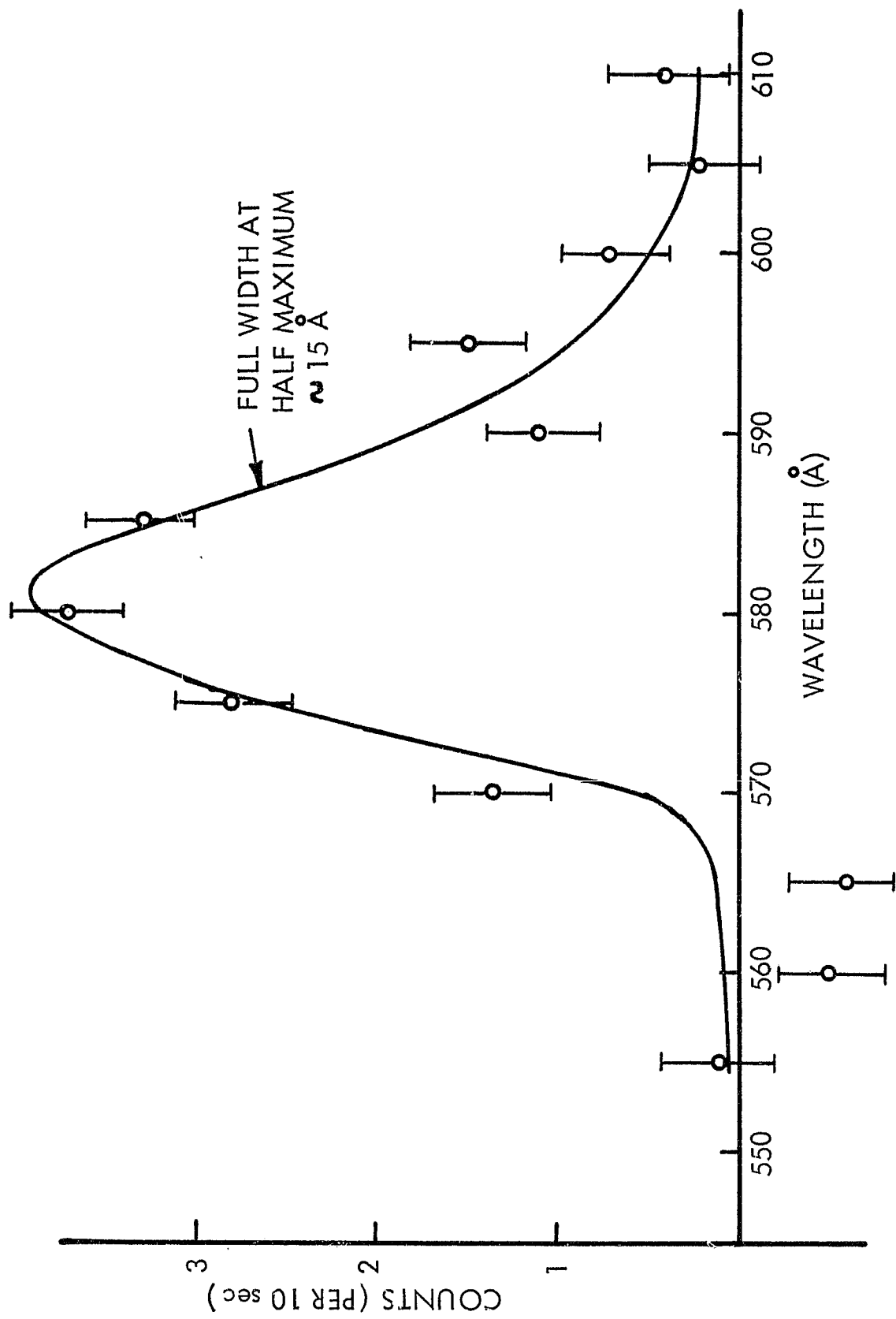584-Å radiation; 15) differential pumping chamber.

FIG. 4. Spectrometer scan of 584-Å transition. Slits ≈ 2 mm.

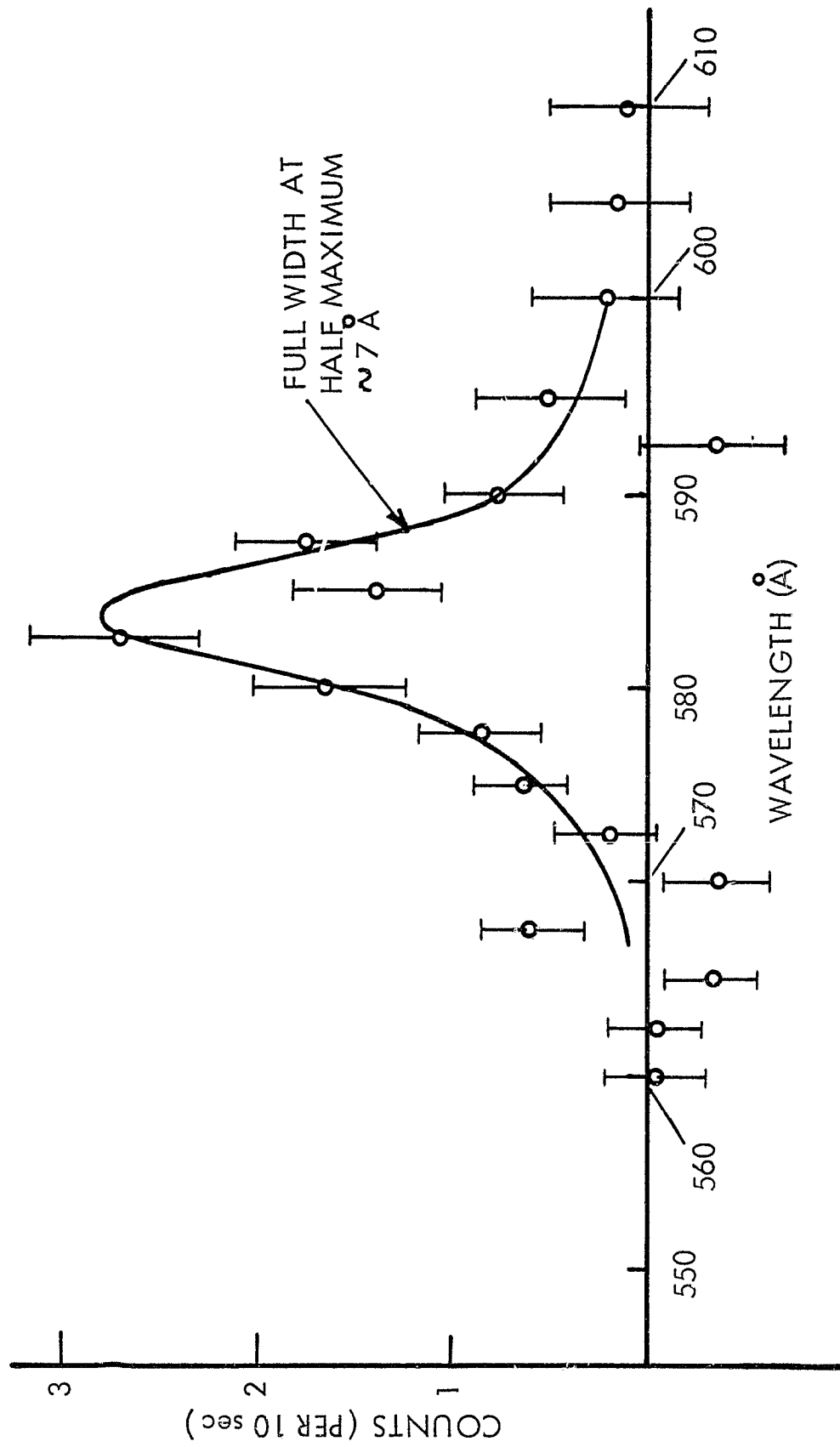FIG. 5.   Spectrometer scan of 584-Å transition.   Slits ≈ 1 mm.

28

The resultant signal vs a wavelength scan on the spectrometer is shown in Fig. 4. Closing the s? ? halfway narrows the width of the line (see Fig. 5), as expected if we are observing true line radiation. The spectrometer resolution was previously calibrated with a He discharge, and this calibration agrees well with our data. On the basis of these results, we feel confident that we have observed 584-Å radiation resulting from low-energy He^+ - He collisions.

Program for the next interval: We will try to observe the 584-Å signal with a beam containing only ground-state He^+, and to study this signal as a function of energy.

(1) CRL Progress Report, October 31, 1967, p. 33.

(2) S. Dworetsky et al., Phys. Rev. Letters 18, 939 (1967).

---

2. Ion-Photon Coincidence in Inelastic Scattering*
   (R. Smick, W. W. Smith)

A new ion-beam apparatus is nearly completed for the purpose of studying the detailed kinematics of low-energy ion-atom excitation processes. The initial experiment will permit the determination of the inelastic energy loss for a 50-1000 eV ion beam scattering from a gas target at a fixed angle. Photons emitted as a consequence of excitation of a specific state of the target are detected in delayed coincidence with the scattered ions. (See Ref. 1 for signal-to-noise calculation.)

We have completed all design, and all parts except the mounts for the optical system have been fabricated. A schematic diagram showing the general design of the apparatus is given in Fig. 6. The complete vacuum system and control unit, the ion source and ion lenses, and the energy analyzer have been assembled, and we have successfully performed preliminary tests of the main
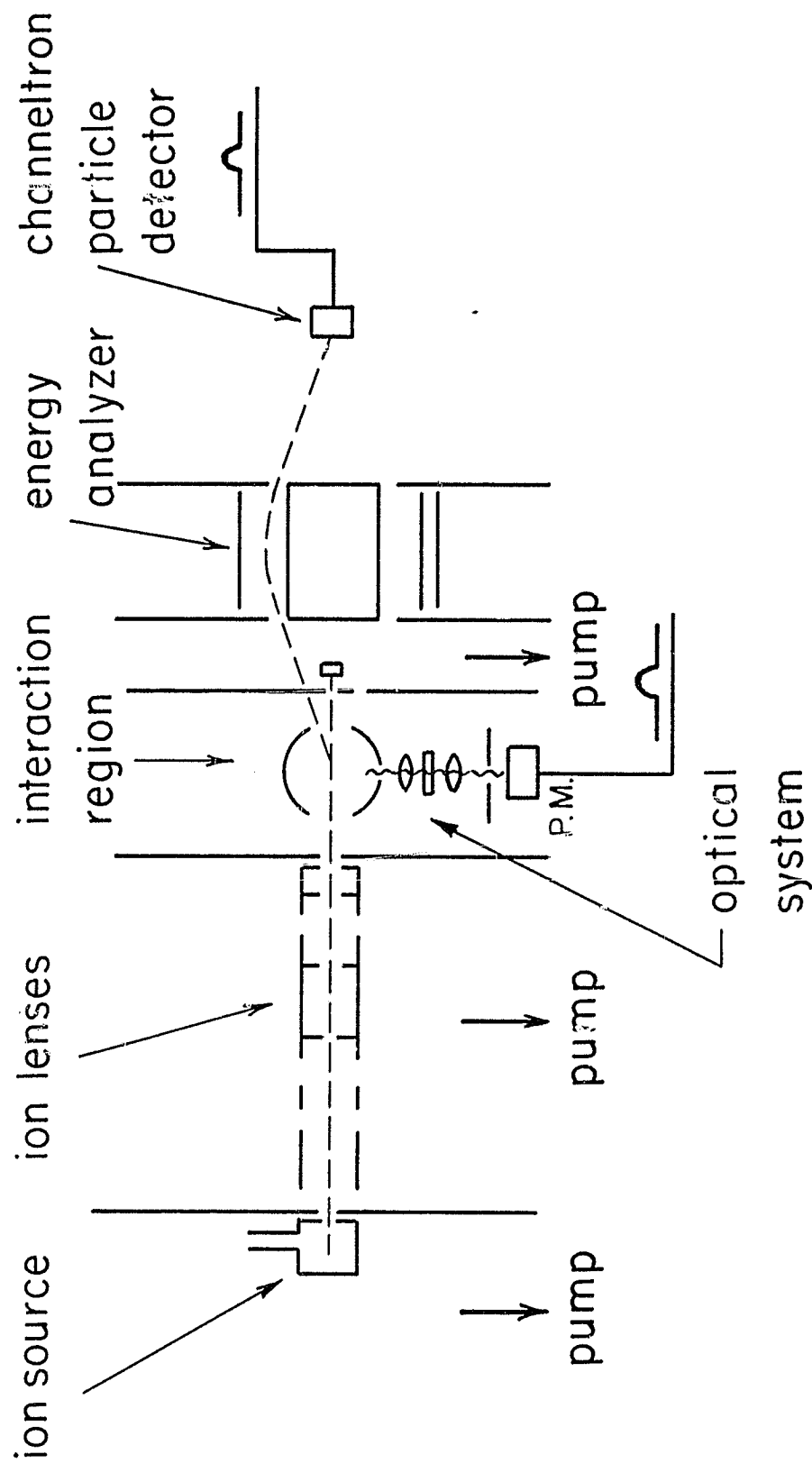
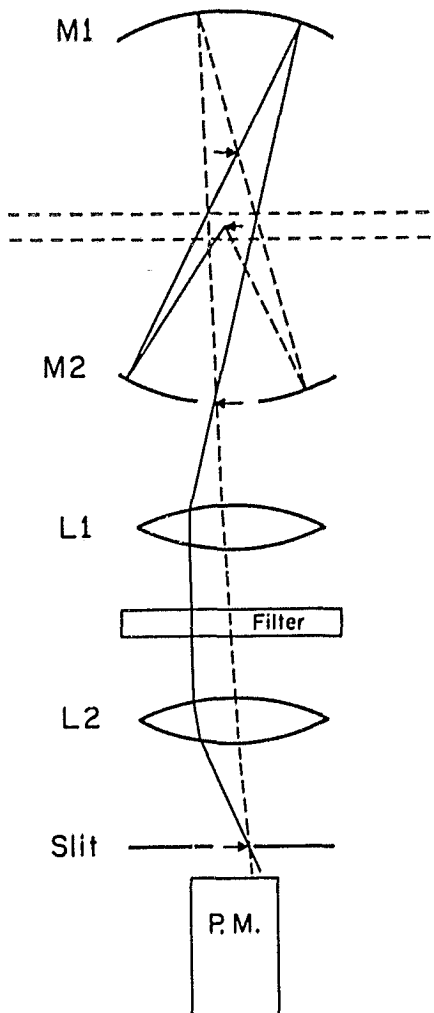FIG. 6.   Schematic diagram of apparatus.

ion source   ion lenses   interaction region   energy analyzer   channeltron particle detector

pump   pump   pump   pump

optical system   P.M.

FIG. 7. Diagram of the optical system showing imaging properties.

M_1, M_2 = spherical mirrors

C_1 = center of curvature of mirror 1

C_2 = center of curvature of mirror 2

L_1, L_2 = lenses

I_1, I_2, I_3 = images

Light rays emitted from O toward the right are reflected by M_2 to form an enlarged image at I_1, and are then reflected by M_1 to form a further enlarged image at I_2. Lenses L_1 and L_2 transfer the image at I_2 to I_3, the plane of the slit, and provide a region of nearly parallel rays through the inter-ference filter. Light emitted to the left would first be reflected by M_1 to form an image above C_1, and would then proceed as does light emitted to the right. If O had been outside the region for ion scattering into the energy analyzer, light from O would have been blocked by the slit.
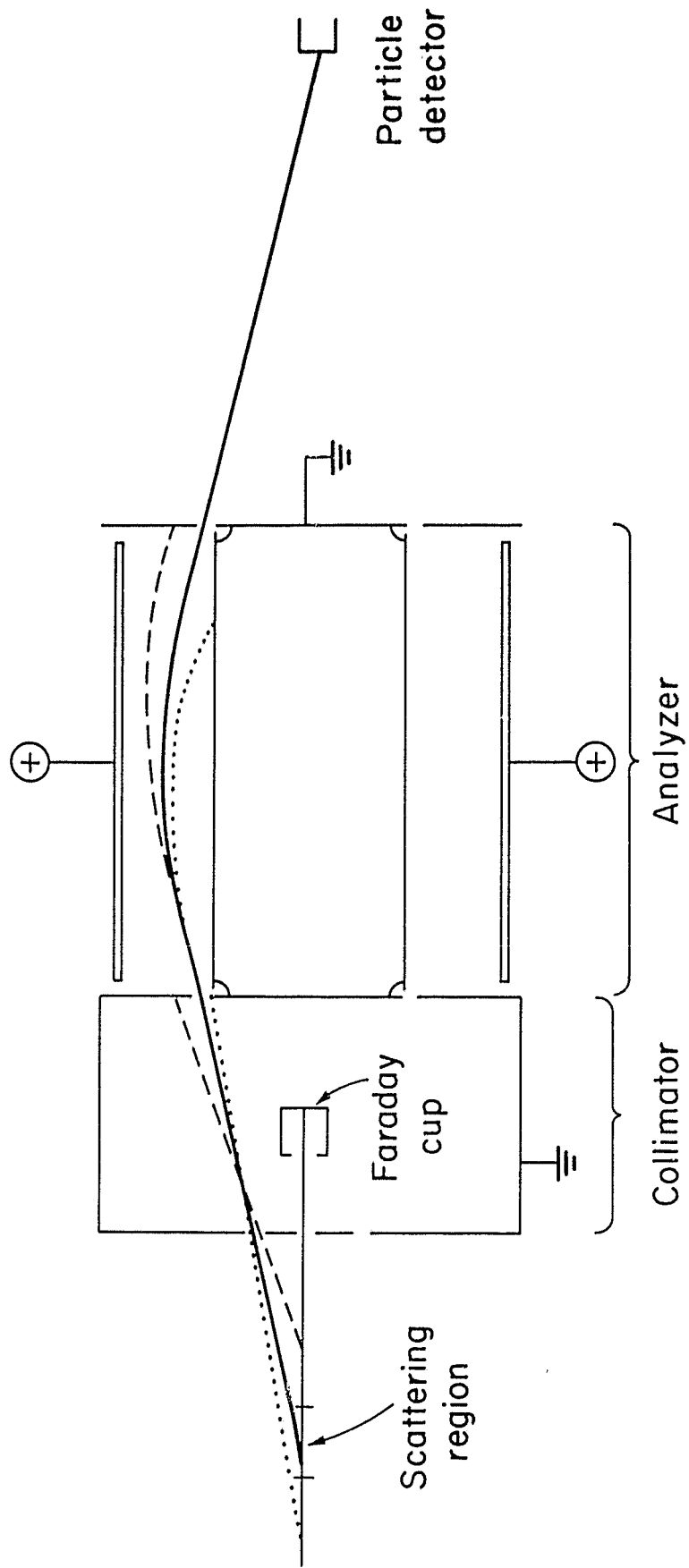
FIG. 8.   Schematic diagram of energy analyzer assembly. The collimator section transmits only particles scattered from a certain length along the beam at a specific angle and are designated by trajectories 3, 4, and 5, while trajectories 1 and 2 fail to pass through slit B. In the analyzer section, trajectories are bent according to particle energy, so only trajectory 5, representing the path of a scattered particle with the correct energy, passes through slit C.

parts of the system with the exception of the energy analyzer.
The energy-spread characteristics of the ion-source ion-lens
combination have been measured, and beam spreads of 2 eV are
easily obtained.

In order to make high-resolution measurements in a reason-
able time, we have designed an optical system which will gather
as much light as possible from the "coincidence volume," and as
little as possible from outside it. Light from the atoms excited
along a specified length of the beam is imaged on adjustable
slits in front of the photomultiplier. The imaging system is
designed to permit an interference filter to be inserted at a
position where the collected light rays are almost parallel.
(A monochromator can be used in place of the interference filter,
slits, and photomultiplier.) The optical system consists of two
spherical mirrors (one with a hole cut in the center) and two
high-speed lenses arranged as shown in Fig. 7.

The cylindrical electrostatic analyzer for the ions scat-
tered through a fixed angle is shown schematically in Fig. 8.
The design used here is our own; however, similar analyzers and
their properties have been discussed previously in the litera-
ture.[2] The primary purpose of the analyzer is to eliminate
elastically scattered ions while transmitting and efficiently
refocusing the inelastically scattered ions. The inelastic
energy loss in a collision event is determined primarily by wave-
length analysis of the emitted photon.

Program for the next interval: First, we will test the
energy analyzer under experimental conditions; we will then try
to observe differential inelastic scattering of He^+ on He with
the new technique.

(1) CRL Progress Report, April 30, 1968, p. 29.

(2) V. V. Zashkvara, M. I. Korsunskii, and O. S. Kosmachev, (in translation) Sov. Physics-Technical Physics, 11, 96 (1966); H. Z. Sar-el, Rev. Sci. Inst. 38, 1210 (1967).

3. Relaxation of Excited Atoms[*]
(B. R. Bulos, W. Happer)

The quenching of optically excited atoms by foreign gases can greatly improve the efficiency of optically pumped devices by eliminating the fluorescently scattered light and the concomitant depumping of the atoms. The quenching mechanism itself is of considerable interest since wide variations in quenching cross sections occur for different gases. Unfortunately, there are few data on the quenching of the atomic species commonly employed in optical pumping experiments. We have therefore undertaken a systematic experimental study of the quenching of excited alkali atoms.

Our experimental method makes use of the optical pumping of alkali vapors. The attenuation of a light beam in a vapor is a measure of the rate of production z of excited atoms. Let us denote the number of excited atoms in the vapor by N_e. Then

$$z = N_e(\Gamma + \Gamma_Q) \quad . \tag{1}$$

Here Γ is the natural radiative decay rate of the excited state and Γ_Q is the quenching rate of the excited state. If the quenching is due to binary collisions between the excited atom and the foreign gas molecule, the quenching rate will be proportional to the foreign gas pressure p.

$$\Gamma_Q = qp \quad . \tag{2}$$

The quenching constant q can be interpreted in terms of a velocity-averaged quenching cross section σ.

$$\sigma = (kT\mu/2)^{1/2}q \quad . \tag{3}$$

Here μ is the reduced mass of the binary system which is composed of the alkali atom and the foreign gas molecule.

A change in the rate of production of excited atoms may be caused by inducing magnetic resonance in the atomic ground state.

The corresponding change in intensity of the transmitted light would be

$$\Delta I_A = a \, \Delta z = a \, \Delta N_e (\Gamma + qp) \quad . \tag{4}$$

Here a is a constant which depends on the sensitivity of the photodetector and on the gain of the recording circuits.

The rate of emission of fluorescent light into all solid angles is ΓN_e. However, the intensity distribution of the fluorescent light may be quite anisotropic. The degree of anisotropy will depend on the polarization of the pumping light, on the foreign gas pressure, and on the degree of optical pumping of the ground state. Because of the anisotropy of the fluorescent intensity, a measurement of the fluorescent light emitted into the small solid angle subtended by a photomultiplier is not necessarily proportional to the decay rate of the excited state. The effects of the anisotropic intensity distribution can be avoided by pumping with axially symmetric, circularly polarized light and by observing fluorescent light of the appropriate linear polarization. When due precautions are taken with respect to the anisotropy, the fluorescent light intensity I_B scattered into a photodetector at right angles to the pumping beam is

$$I_B = b\Gamma N_e \quad . \tag{5}$$

The constant $\underline{b}$ depends on the solid angle subtended by the photomultiplier and on the gain of the recording system. The change in the fluorescent light intensity when magnetic resonance is induced is

$$\Delta I_B = b\Gamma \Delta N_e \quad . \tag{6}$$

The ratio of the transmission signal ΔI_A to the fluorescent signal ΔI_B is then

$$\frac{\Delta I_A}{\Delta I_B} = \frac{a}{b}(1 + \frac{q}{\Gamma} p) \quad . \tag{7}$$

35

The ratio $\Delta I_A / \Delta I_B$ can be easily measured experimentally, and a plot of $\Delta I_A / \Delta I_B$ as a function of pressure yields a straight line. The ratio of the slope of the straight line to the intercept with the vertical axis yields the ratio q/Γ of the quenching constant to the natural decay rate Γ of the excited state. Since Γ is a well-known experimantal quantity, one can use the experimentally determined ratio q/Γ to determine q, and, using Eq.(3), one can determine the quenching cross section.

Our experimental method has the following advantages. The apparatus and the electronics are simple. The measurements can be easily and quickly performed. The effects of the aniso-tropic fluorescent light intensity are eliminated. Broadening of the absorption profile of the atoms cannot be mistaken for quenching since the rate of production of excited atoms is meas-ured directly by observing changes in the intensity of the transmitted beam. The sensitivity of the photodetectors need not be known, nor is it necessary to know the solid angle sub-tended by the detector of fluorescent light. Instrumentally scattered light is eliminated by observing signal changes which result from magnetic resonance in the ground state. The measure-ments are independent of alkali vapor density as long as the vapor is optically thin.

Program for the next interval: We intend to measure the quenching cross sections of all of the commonly used buffer gases for both the $^2P_{3/2}$ and $^2P_{1/2}$ excited states of the alkali atoms. We shall look for systematic features in the experimental data; for instance, is there a significant difference in the quenching cross sections of $N_2{}^{15}$ and $N_2{}^{14}$ or of H_2 and D_2? We shall in-vestigate possible theoretical models for quenching and determine which ones are most consistent with the observed quenching rates.

4. Study of Electron Impact Excitation of Atoms by a Coincidence Technique*
(M. Eminyan, M. Levitt)

In the past few years a considerable number of papers[1] were published concerning the polarization of atomic line radiation produced by electron impact excitation. Much of this work has failed to yield unambiguous values of the threshold polarization. In particular, measurements of the polarization of the Lyman α line[2] have such low precision for the low-energy excitation that it is not possible to obtain the extrapolated value of the threshold polarization.

For helium, early work gives experimental values which are much lower than those predicted by theory just above threshold. An attempt was made to show that the theoretical values were too high,[3] but recent experimental work[4,5] indicates that there is a large increase in polarization P in the last few tenths of a volt above threshold, so that P approaches the theoretical value predicted by the conservation of angular momentum.

In all the experiments performed up to the present, it has not been possible to obtain the value of polarization precisely at threshold because of the finite energy spread ($\gtrsim 0.05$ eV) of the exciting electron beam. A proposed new method[6] in which a coincidence technique is used to eliminate this difficulty will enable us to measure the exact value of the threshold polarization.

This technique is based on the fact that the coincidence process of impact excitation above threshold is related to the threshold polarization. We can define the coincidence process of the impact excitation simply: An electron of energy E excites an atomic level with the threshold energy E_0; the inelastically scattered electron of energy $E - E_0$ and the photon of energy $E_0 = h\nu$ are observed in coincidence. We now consider the special case of inelastic forward scattering of the colliding electrons

and attempt to determine the probability of finding the emitted photon of the excited atom in an angle range $\Delta\omega$ around the observation angle ω. Since the coulomb and exchange interactions are by far the largest interactions (spin-orbit and spin-spin interactions are very small by comparison), the angular momentum conservation law can be applied separately for orbit and spin angular momenta of the projectile and target particles:

$$m_\ell + M_\ell = m_\ell' + M_\ell' \quad , \tag{1}$$

$$m_s + M_s = m_s' + M_s' \quad , \tag{2}$$

$$m_I = M_I' \quad . \tag{3}$$

M_ℓ and M_s or M_ℓ' and M_s' are the orbital and spin angular momentum components (related to the axis of the incoming electrons) of the incoming or outgoing electrons before or after the collision process; m_ℓ and m_s or m_ℓ' and m_s' are the orbital and spin angular momentum components of the atomic electron (or the sum of these quantities in the case of more than one outer electron) before or after the collision; and m_I and m_I' are the nuclear spin angular momentum components. From a consideration of the process of inelastic forward scattering of the electron, it follows that $M_\ell = M_\ell' = 0$, or according to Eq. (1), $m_\ell = m_\ell'$; that is, the selection rule $\Delta m_\ell = 0$ should be valid for the case of the forward scattering process. In other words, the inelastic forward scattering is governed by the same selection rule as the excitation at the threshold energy. Accordingly, the angular distribution of the emitted photons (and the polarization) should be the same for both processes.

Based upon the selection rule $\Delta m_\ell = 0$ and the well-known intensity relations of spectral lines, Fig. 9 shows the calculated angular correlation between the inelastically scattered electrons in the forward direction and the emitted photons for the following
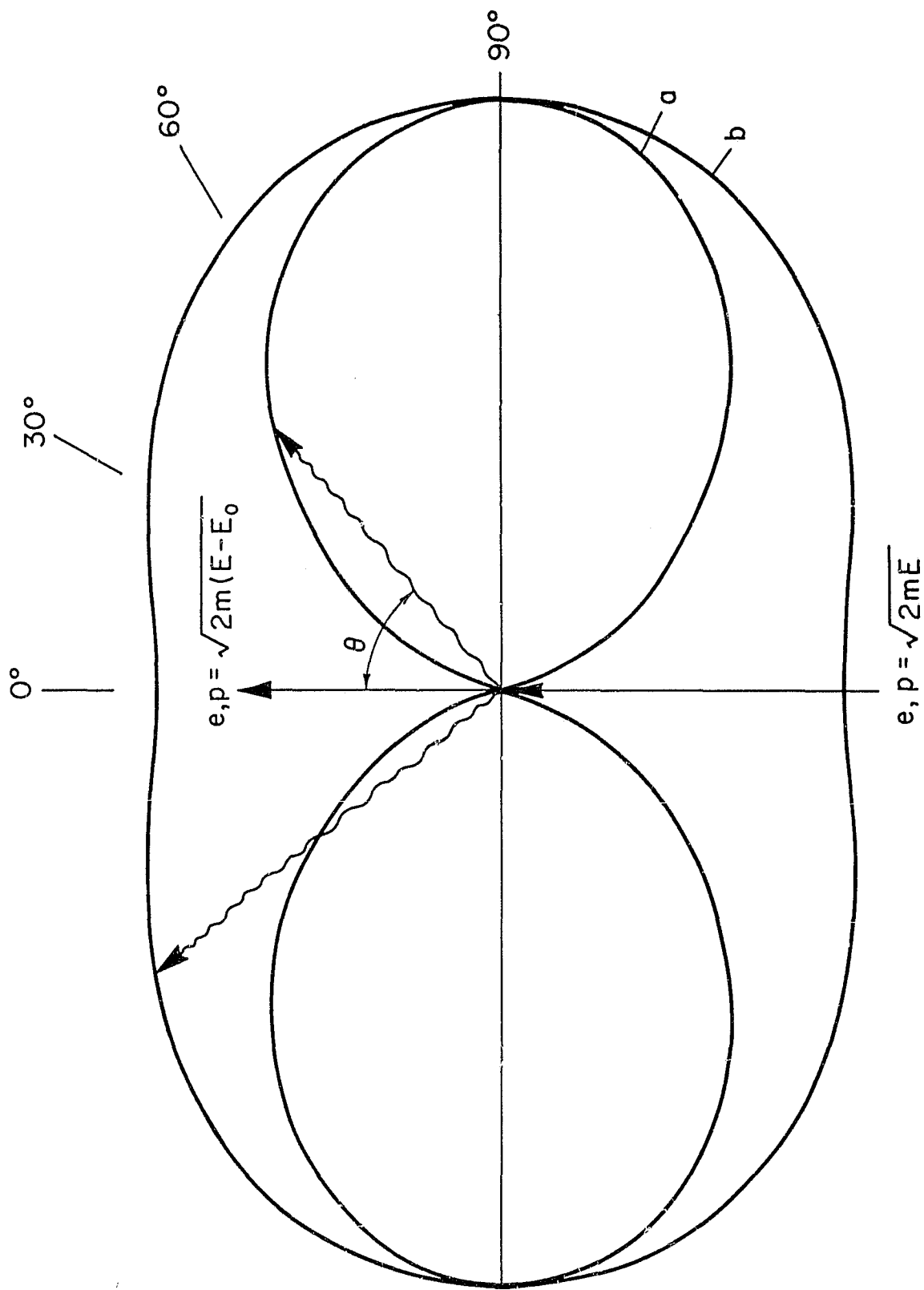
FIG. 9. Angular correlation between the electron inelastically scattered in the forward direction (e,p) and the emitted photon (p = $[2m(E - E_0)]^{\frac{1}{2}}$ linear momentum of the electron after the excitation, where E = energy of the incoming electron, E_0 = threshold energy for the excitation of the spectral line). The radius vector to the angular functions represents the probability of finding the photon in coincidence with the electron inelastically scattered in the forward direction for the following cases: a) helium singlet resonance lines (transition $n^1P - 1^1S$); b) Lyman lines of atomic hydrogen.

line excitations: a) excitation of the helium resonance lines (transitions n^1P to 1^1S), and b) excitation of Lyman lines (transitions from the states nP to $1S$). Within the validity of the above assumptions, the angular correlation between the forward scattered electrons and the photons is independent of the primary energy of the electrons. The angular distribution of the photon radiation corresponds to a polarization (related to the forward direction) of 100% (case a) and of 42.9% (case b). Hyperfine-structure interactions have not been taken into account for case b) because their influence is negligible (the polarization is diminished by not more than 1%). No hyperfine-structure influence is expected for case a) when we consider the resonance lines of He^4 (nuclear spin zero). In practice, the polarization can be obtained by measuring the amplitude of the correlation function, $I(\theta)$, at two arbitrary angles and by using the expression

$$P = 100(1 - R)/(\cos^2\theta_1 - R\cos^2\theta_2) \quad , \qquad (4)$$

where $R = I(\theta_1)/I(\theta_2)$.

Aside from the fact that the angular correlation of the forward scattering process is directly related to the threshold polarization, the observation of the excitation coincidence process makes possible a great many interesting experimental investigations. For example, since our technique eliminates the energy dependence of P for a pure coulomb interaction, any measured change of P with excitation energy can be related to such effects as spin-exchange excitation[7] or narrow resonances. Such resonances have been observed in H [8] and He.[9,10] Also, the use of the coincidence technique eliminates cascading when the particle detection device contains an analyzer to determine the loss of energy of inelastically scattered electrons. This feature thus permits the measurement of the energy dependence of the differential cross section for excitation of radiating atomic
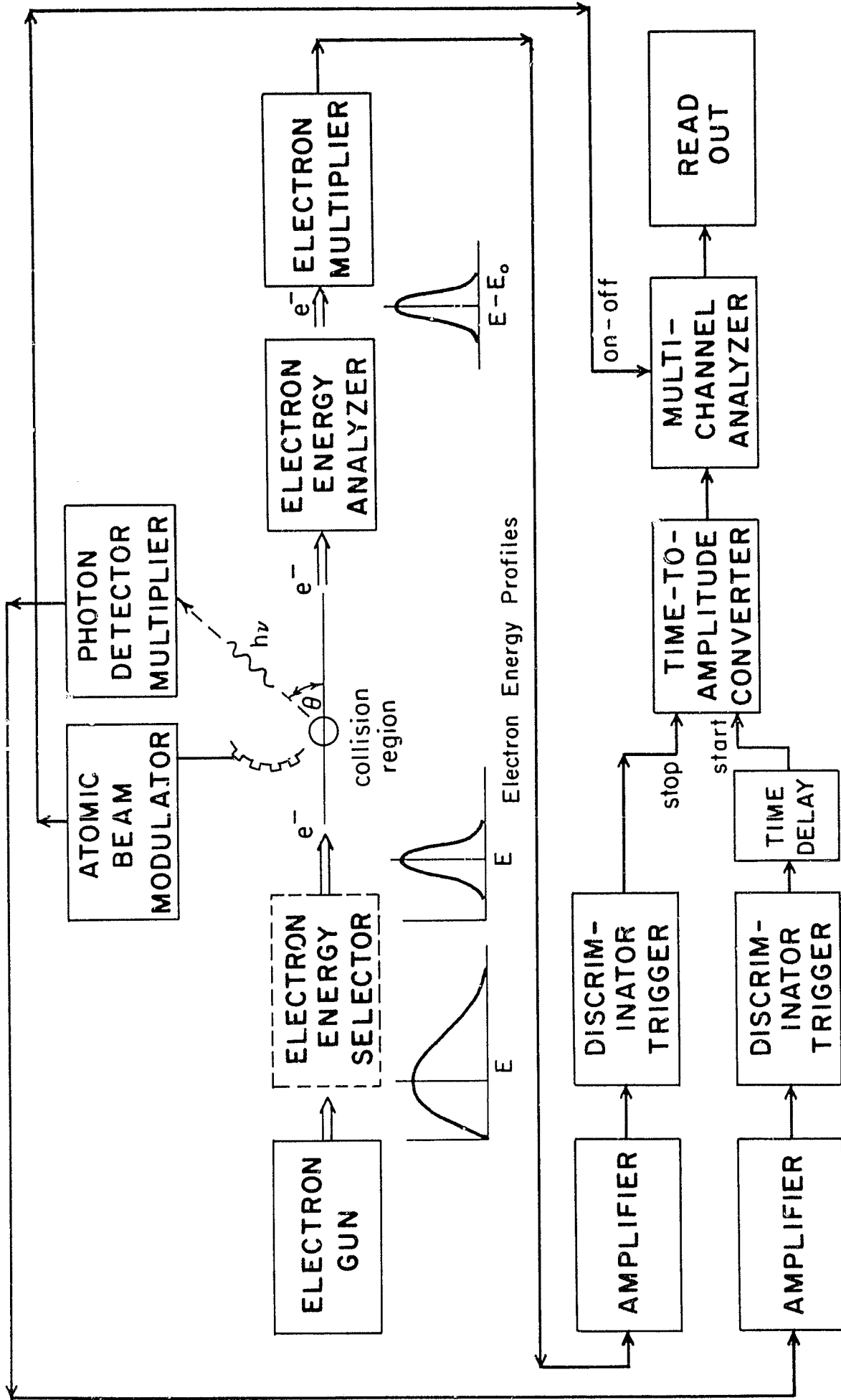
FIG. 10. Block diagram of coincidence experiment.

states. Lastly, the use of single-particle detection of de-excitation radiation will allow us to make measurements on many uv lines (e.g., He $3^1P \rightarrow 1^1S$) not previously studied. The apparatus planned for these experiments is outlined in Fig. 10. Since construction has just been started, a comprehensive description of the performance of various components will be given in the next report.

(1) Partial bibliography given by B. L. Moiseiwitsch and S. J. Smith in Rev. Mod. Phys. 40, 238 (1968).

(2) W. L. Fite, W. E. Kauppila, and W. R. Ott, Fifth International Conference on the Physics of Electronic and Atomic Collisions, Leningrad, USSR, 1967, p. 534.

(3) Lue-Yung Chow Chiu, Phys. Rev. 168, 32 (1968).

(4) D. W. O. Heddle and R. G. W. Keesing, Proc. Roy. Soc. (London) A299, 212 (1967).

(5) R. H. McFarland, Phys. Rev. 156, 55 (1967).

(6) H. Kleinpoppen (private communication).

(7) R. H. McFarland and M. H. Mittleman, Phys. Rev. Letters 20, 899 (1968).

(8) J. W. McGowan, to be published.

(9) G. E. Chamberlain and H. G. M. Heideman, Phys. Rev. Letters 14, 581 (1965).

(10) H. Ehrhardt, L. Langhans, and F. Linder, Z. Physik 214, 179 (1968).

D. ATOMIC FREQUENCY STANDARDS

1. Interaction of Light with Atomic Vapors
(B. R. Bulos, W. Happer, H. Y. Tang)

During this interval we have observed the intensity modulation of light which has passed through a vapor of Rb^{87} atoms, coherently oscillating on the 0-0 ground-state hfs transition. The mechanism of this effect can be understood by the following

simplified model. Let us represent the electric field $\vec{E}$ of a
quasi-monochromatic light wave by

$$\vec{E} = \vec{\mathcal{E}} \exp i(\vec{k}\cdot\vec{r} - \omega t) + c.c. \quad , \qquad (1)$$

where c.c. denotes complex conjugate. We require that the ampli-
tude $\vec{\mathcal{E}}$ remain essentially constant over the distance of an opti-
cal wavelength and over the period of an optical oscillation.
The electric field will induce a dielectric polarization $\vec{P}$ in
the medium.

$$\vec{P} = \vec{p} \exp i(\vec{k}\cdot\vec{r} - \omega t) + c.c. \qquad (2)$$

The polarization amplitude $\vec{p}$ is related to the electric-field
amplitude $\vec{\mathcal{E}}$ by

$$\vec{p} = \langle \chi \rangle \vec{\mathcal{E}} \quad , \qquad (3)$$

where the susceptibility dyadic $\langle \chi \rangle$ is the expectation value of
the susceptibility operator χ. If hfs coherence has been pro-
duced by a microwave field of frequency ω_m, the hfs component of
the oscillating magnetic dipole moment of the atoms will be of
the form

$$\langle \vec{\mu} \rangle_{hfs} = \vec{\mu}_1 \exp(-i\omega_m t) + c.c. \qquad (4)$$

The associated susceptibility will be

$$\langle \chi \rangle_{hfs} = f_a \exp(-i\omega_m t) \vec{\mu}_1 x + f_b \exp(i\omega_m t) \vec{\mu}_1^* x \quad , \qquad (5)$$

where f_a and f_b need not be equal.

Suppose that the initially monochromatic light beam
propagates along the z axis of the system and passes through a
slab of vapor which fills the space $0 \le z \le \ell$. On the assump-
tions that the moments $\vec{\mu}_1$ of the vapor are all equal and parallel
to the z axis and that the atomic density is low enough that the
slab of vapor is optically thin, the electric field $\vec{E}$ of the
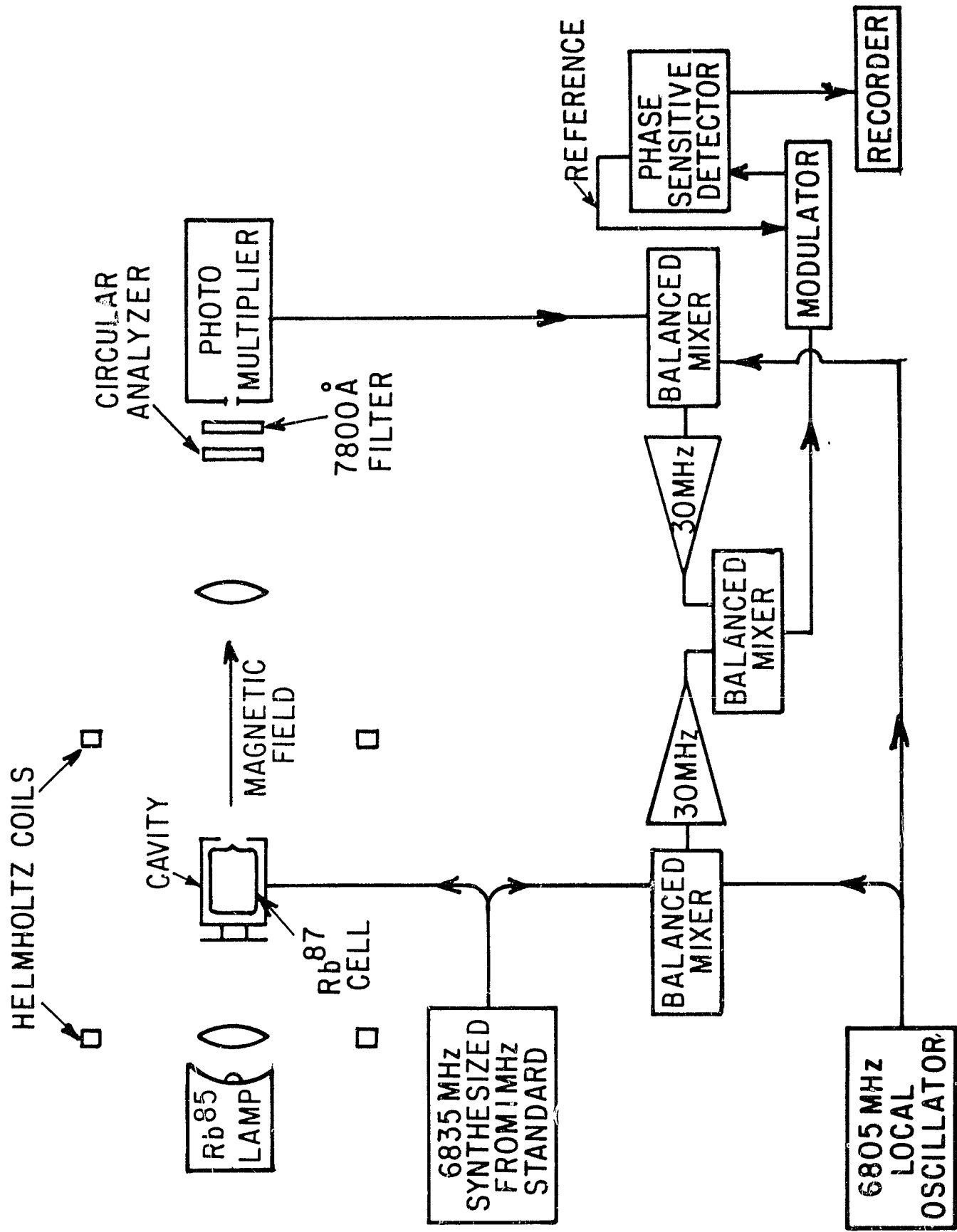transmitted light beam will have the form
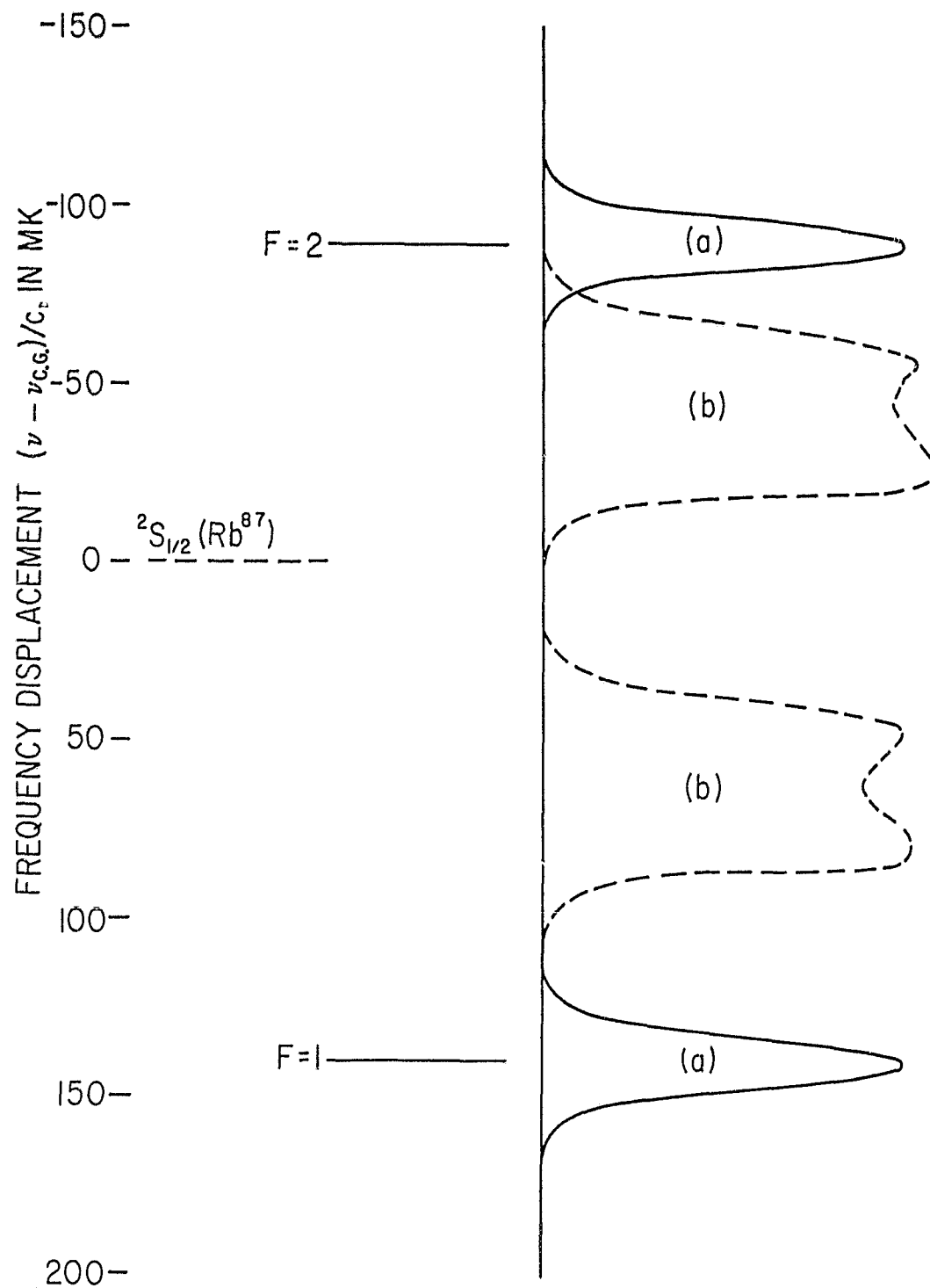
FIG. 11. The experimental apparatus.

FIG. 12. The optical absorption lines of (a) Rb-87,
          and a typical spectral profile of (b) a
          Rb-85 lamp.

45

$$\vec{E} = \vec{e}_o \exp i(2\pi\ell k\langle\chi\rangle_{sc}) \exp i(kz-\omega t)$$

$$+ 4\pi \left(\frac{\lambda_m}{\lambda}\right) \sin\left(\frac{\pi\ell}{\lambda_m}\right) \left\{ f_a(\omega)\vec{\mu}_1 \times \vec{e}_o \exp i\left[(k+k_m)z - (\omega+\omega_m)t\right]\right.$$

$$\left. + f_b(\omega)\vec{\mu}_1^* \times \vec{e}_o \exp i\left[(k-k_m)z - (\omega-\omega_m)t\right]\right\} \quad . \qquad (6)$$

The first term in (6) describes the carrier beam, which has been attenuated and phase-shifted by an amount $\exp i(2\pi k\ell\langle\chi\rangle_{sc})$. Here $\langle\chi\rangle_{sc}$ is the scalar susceptibility of the vapor. The remaining terms represent a sideband at angular frequency $\omega + \omega_m$ and a sideband at angular frequency $\omega - \omega_m$.

From Eq. (6) one can see that the light intensity $\vec{E}\cdot\vec{E}$ will be modulated at the hfs frequency ω_m. The amplitude of the modulation will be proportional to $\vec{\mu}_1\cdot(\vec{e}_o\times\vec{e}_o^*)$. Since $(\vec{e}_o\times\vec{e}_o^*)$ is proportional to the average photon spin, intensity modulation can only be observed if some degree of circular polarization is present in the light.

The above discussion may be extended to light with broad spectral profile by considering such light as an ensemble of monochromatic light waves with random phases.

A schematic diagram of the experimental apparatus is shown in Fig. 11. A Rb^{87} filled cell was placed in a microwave cavity tuned to resonate at 6.835 GHz in the TE_{011} mode. A beam of Rb^{85} resonance radiation passed through the vapor and pumped the Rb^{87} atoms into the lower hfs level (see Fig. 12). A small static magnetic field along the axis of the cavity removed the degeneracy of the hfs transitions. The F = 2, m = 0, and F = 1, m = 0 sublevels of the Rb^{87} ground state were coupled by the microwave field of the cavity. The emerging light from the cavity passed through a circular analyzer and a D-line interference filter. The light intensity was then detected by a crossed-field photomultiplier tube which has a current gain on the order of 50 dB
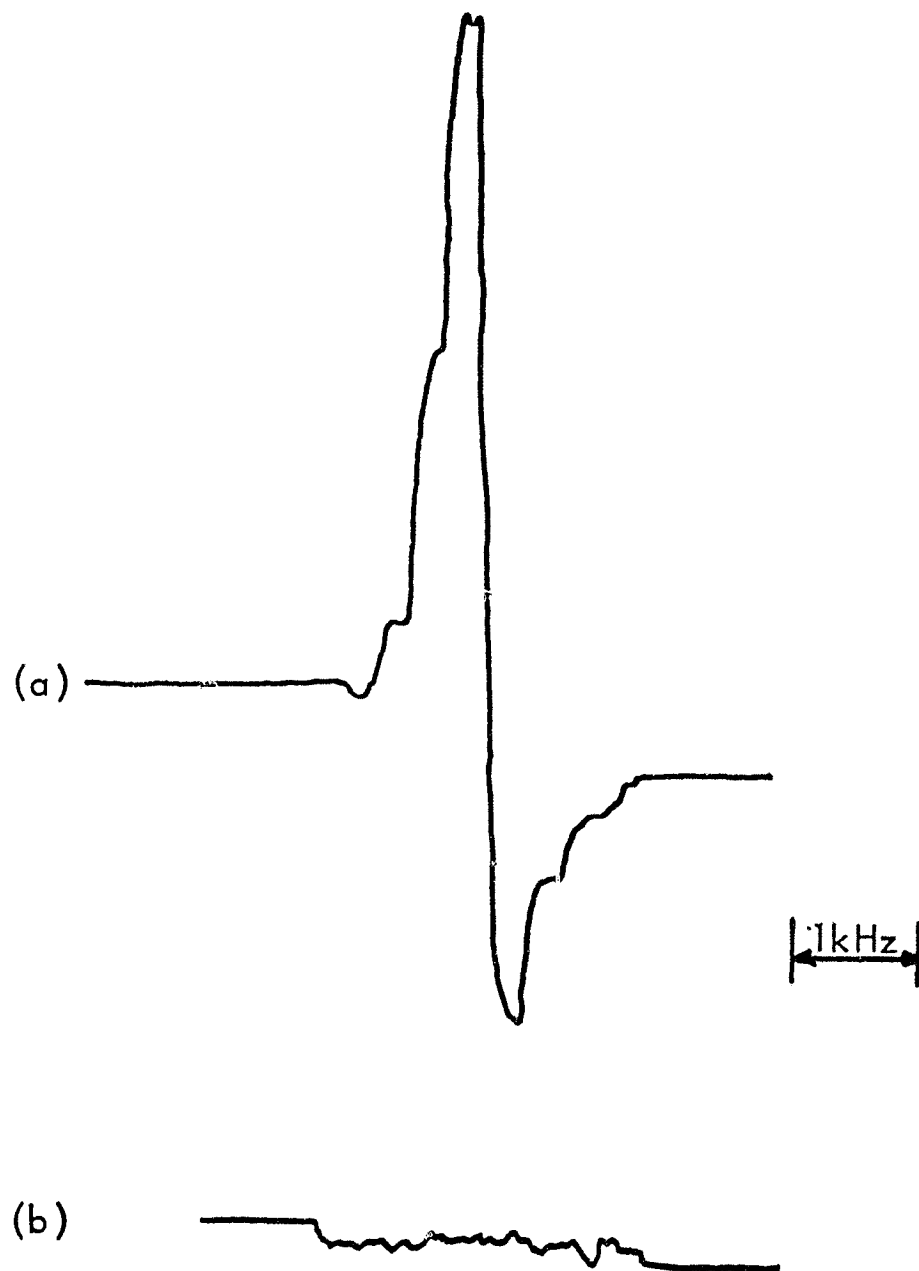
(a)

(b)

|·1kHz|

FIG. 13. Typical 6.835-GHz light modulation signals for
7800-Å D_2 Rb-85 light: a) with circular analyzer
in place; b) without circular analyzer. The
vertical scale is the output of the 30-MHz
balanced mixer in arbitrary units.

47

and a bandwidth on the order of 10 GHz. The output of the photo-
tube was mixed with a 6.805-GHz signal from a local oscillator.
The 30-MHz difference frequency signal was amplified and mixed
with a 30-MHz reference signal. The resulting dc signal was
amplified and recorded while the microwaves exciting the cavity
were swept in frequency through the hfs resonance of the Rb^{87}
atoms. A typical signal for 7800-$\overset{\circ}{A}$ D_2 light is shown in Fig. 13a.
Similar signals were observed with 7947-$\overset{\circ}{A}$ D_1 light and also with
isotope-filtered Rb^{87} light. The signal in Fig. 13b, recorded
with the circular analyzer removed, shows that unpolarized light
is not modulated, which is in agreement with theory. The index
of modulation was observed to be between 10^{-3} and 10^{-4}, which is
also in agreement with theoretical estimates.

Program for the next interval: We plan to continue with
our theoretical and experimental studies of light propagation in
optically pumped vapors.

---

2. Rb^{85} Maser
    (R. Novick, W. A. Stern)

The Rb^{85} maser oscillator discussed in the last report[1]
was completed and assembled. This oscillator will operate in the
TE_{021} mode at a frequency of 3035 MHz and has a vacuum-tight
copper-plated stainless-steel cavity. A conventional vacuum
system was used to achieve pressures of the order of 10^{-6} Torr
in the cavity. When the cavity is closed to the vacuum station,
the rubidium metal reacts with the residual gases in the cavity
and reduces the pressure to less than 10^{-9} Torr.

Detailed studies were made of the filtering of Rb^{85} light
by Rb^{87} vapor buffered with helium. Figure 14 shows the ground-
state hyperfine levels in Rb^{85} and Rb^{87}. As shown in the diagram,
the highest lying F = 3 hyperfine ground-state level in Rb^{85} is
very close to the highest lying F = 2 ground-state hyperfine
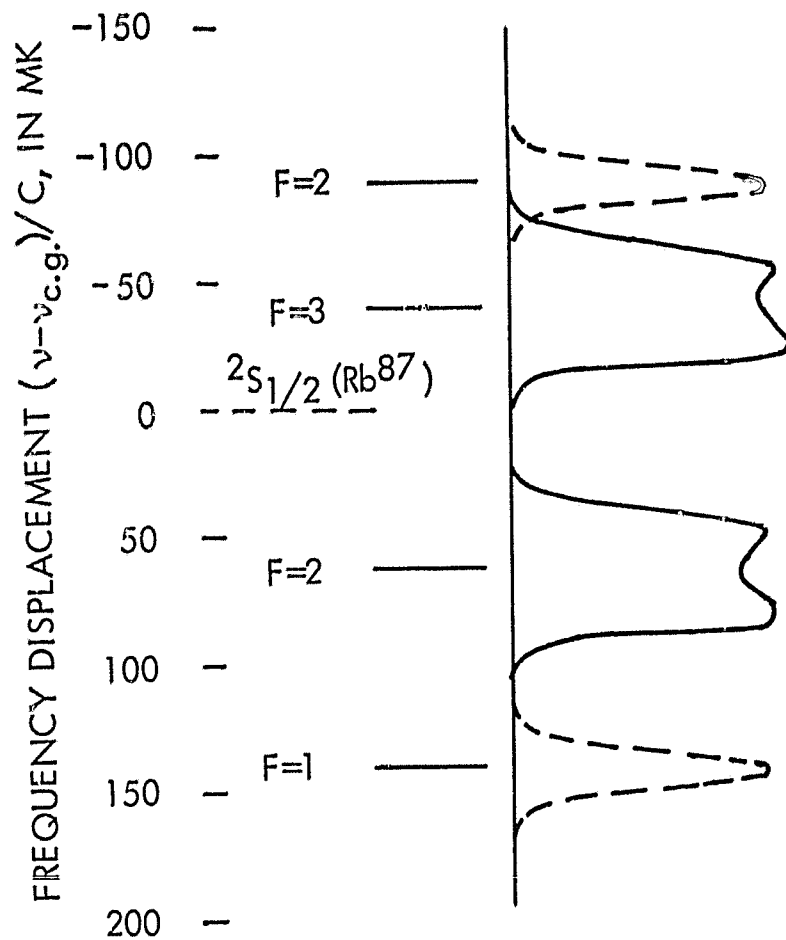
48

FIG. 14.   Ground-state hyperfine levels
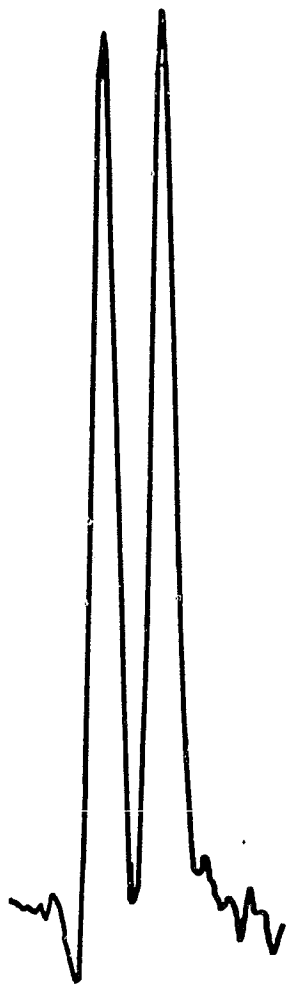   in Rb-85 and Rb-87.

FIG. 15

Scan of the filtered Rb-85
7949-Å line at a Rb-87
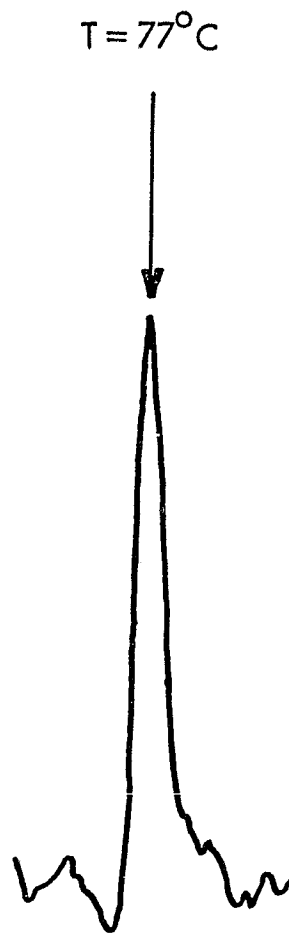filter-cell temperature of
40.5°C.

FIG. 16

Scan of the filtered Rb-85
7949-Å line at a Rb-87
filter-cell temperature of
77°C.

level in Rb^{87}. With proper pressure shifting and broadening, the $F = 2$ absorption line in Rb^{87} can be made to filter the unwanted $F = 3$ emission line in Rb^{85}, thereby resulting in a Rb^{85} emission spectrum of the $F = 2$ line alone. A high finesse, 2-in. piezo-electrically scanned Fabry-Perot interferometer was used for these studies.

Figure 15 shows a scan of the filtered Rb^{85} 7949-Å line at a Rb^{87} filter-cell temperature of $40.5°C$. Both hyperfine components of Rb^{85} are present, since at this temperature sufficient shifting and broadening have not occurred. Figure 16 shows a scan of the 7949-Å line at a filter-cell temperature of $77°C$. Here the unwanted $F = 3$ Rb^{85} hyperfine line disappears, while the desired $F = 2$ hyperfine line is attenuated by 62%.

Program for the next interval: The Rb^{85} maser will be operated in the oscillatory mode and will be used as a tool to study light modulation in the ground state; frequency shifts due to pumping light, buffer gas, and cavity pulling; and finally the quenching mechanism in the Rb^{85} system.

(1) CRL Progress Report, April 30, 1968, p. 43.

II. PHYSICS OF MOLECULES

A. ELECTRON EXCITATION OF MOLECULAR HYDROGEN*
   (P. Cahill)

The polarization of the light emitted in six rotational vibrational transitions of the Fulcher band system of H_2 has been measured, as a function of the energy of the exciting electrons, at 0.2 eV intervals. For the para, $N = 2$, Q-branch transition, which is unperturbed by neighboring electronic states, a threshold polarization of 12% was determined where the intensity of light perpendicular to the electron beam was greater than the corresponding parallel component. These results will soon be submitted for publication.

The Percival-Seaton theory for the polarization of atomic impact radiation is extended to the case of diatomic molecules.[1] Similar to the atomic case, it is shown that for excitation by electron impact involving a change of electronic angular momentum along the molecular internuclear axis, the threshold polarization can be determined from the symmetry of the total molecular wave function without a detailed knowledge of the inelastic cross sections. General expressions were developed for the cases of fine and hyperfine splitting, and explicit relations are obtained for the first two rotational levels of a $^3\Pi_u$ state undergoing a radiative transition to a $^3\Sigma_g$ state where the fine and hyperfine separations are much larger than the natural linewidth. This theory is valid when the radiative state is populated by a direct interaction, and the radiative transition between rotational states is resolved. The experimental results for the unperturbed levels of the $^3\Pi_u$ state are somewhat smaller than those predicted by theory but are of the correct polarization as referenced to the electron beam.

(1)   A. Norman Jette and Patrick Cahill, Phys. Rev. (to be published).

B.   MOLECULAR SPECTRA OF CESIUM[*]
(M. M. Hessel, P. Kusch)

A magnetic rotation spectrum (MRS) of molecular cesium not previously found has been observed in the 7500-Å band system of cesium. Approximately 250 MRS well-defined lines have been measured in the region 7500 - 8300 Å. These lines correlate with the band heads of the absorption spectra. It has been difficult to locate band heads in absorption with precision, almost certainly because these occur at J values for which the thermal population is very low. The MRS lines, therefore, fall much better into the conventional v", v' array than do the absorption heads. This is analogous to the behavior of the MRS spectrum in other alkali molecules (Li_2, Na_2, K_2, Rb_2) observed by Loomis and co-workers.[1,2] A vibrational analysis has been made and is in general agreement with that of Loomis and Kusch[3] for the region 12,300 to 13,300 cm^{-1}. In the low-frequency region ($\nu < 12,300$ cm^{-1}), the bands no longer fit into a good array.

Marginally resolved rotational structure was observed in absorption for the (1,0) vibrational band of the 7500-Å band system. A series of approximately 60 rotational lines were measured and an arbitrary integer n was assigned to each member of the series. A least-squares fit of the observed frequencies ν to an equation of the form

$$\nu = a - bn - cn^2 \qquad (1)$$

fit all 60 observed lines to an RMS error of ± 0.009 cm^{-1}. The identification of n with the true rotational quantum number J cannot be made with the available data. However, the constant c

53

is to a good order of approximation equal to $B''-B'$. We find $c = 0.00104$ cm^{-1}. Equation (1) has a maximum or band head at $\nu = a - b^2/4c = 13074.00$ cm^{-1}. The first of the lines in our series $(n=0)$ occurs at about $J = 67$ if the observed series is a P branch. The extrapolation of this series to a head is a long one, approximately 60 quantum numbers. The frequency of the observed value from the MRS line is 13074.21 ± 0.06 cm^{-1}. in excellent agreement with the value obtained from the long extrapolation of the rotational data.

Program for the next interval: To continue the analysis of the cesium spectrum.

(1) F. W. Loomis and R. E. Nusbaum, Phys. Rev. 40, 380 (1932). See references contained therein.

(2) P. Kusch, Phys. Rev. 49, 218 (1936).

(3) F. W. Loomis and P. Kusch, Phys. Rev. 46, 292 (1934).

C. LASER STUDIES OF MOLECULAR BIREFRINGENCE AND OPTICAL ACTIVITY*

1. Molecular Quadrupole Moments
(R. L. Disch)

Due to a change of personnel, this work has been suspended and will be continued elsewhere.

2. Molecular Magnetic Anisotropy
(R. L. Disch, J. Matuska)

Measurements were completed upon a series of diamagnetic gases, and the results have been prepared for publication.[1] Measurements aimed at elucidating the role of spin-orbit coupling in paramagnetic birefringence are underway elsewhere.

3. Anisotropy of Molecular Optical Rotation
   (R. L. Disch, D. I. Sverdlik)

The second paper in this series is in press,[2] and fur-
ther experimental work is being conducted elsewhere.

(1)   J. A. Matuska and R. L. Disch, "Magnetic Anisotropy
of CO_2, COS, CO, and CH_3F" (to be published).

(2)   R. L. Disch and D. I. Sverdlik, "Apparent Circular
Dichroism of Oriented Systems," Anal. Chem., January 1969 (in
press).

D.   OPTICAL LASER SPECTROSCOPY OF FLUIDS*
     (D. Balzarini, L. R. Wilcox)

A project begun in 1962 at the Columbia Radiation Labora-
tory to explore the applications of lasers to physics is now con-
cluded. Results of technical and scientific importance are re-
ported in earlier progress reports and in formal publications.
In this final report we wish to summarize the project in broadest
perspective.

Development of a Heterodyne Spectrometer

With laser sources typical interference measurements be-
come easy, while some entirely new measurements become possible.
The project began with the construction of a classical interfer-
ometer of the Mach-Zender type. Because the laser is so powerful,
one may plan measurements in which one corner mirror of the inter-
ferometer is replaced by a diffuse scatterer. In interesting
cases, the phase and amplitude of the scattered field fluctuates
in time. Let S(t) be a complex factor which expresses the in-
stantaneous phase and amplitude of the optical field at the
detector relative to the reference beam with which it interferes.
At the output of the interferometer there will be a fluctuating
intensity $i \propto [1 + 2\text{Re } S + |S|^2]$. In applications, $S \approx 10^{-8}$ so

that the last term may be dropped. The small, slowly varying, interference term must be amplified in the presence of the large constant term, and this presented technical problems. To overcome these problems and make an instrument suitable for the study of quasi-coherent scattering, the interferometer was modified by introducing a Debye-Sears modulator into the reference leg of the interferometer. This had the effect of changing Re S into Re $Se^{2\pi i ft}$ so that the interference term is given a high frequency carrier (f = 30 MHz). This was then amplified and demodulated to recover S(t) within bandwidth limitations. Thus, a unique instrument was created for optical scattering studies; i.e., one which extracts the phase and amplitude S(t) of a scattered wave and not simply the intensity $\langle |S|^2 \rangle_{av}$ as hitherto.

Quasi-Coherent Scattering Studies

Applications to physics depend upon the fact that some physically interesting process generates an ensemble of values S(ti) with statistical properties determined by the physics of the process. The simplest, important statistic is the autocorrelation function or power spectrum of S(t). Early in the project it was demonstrated that one might measure the mean-square velocity of micron-size particles undergoing Brownian motion in a fluid medium. The average velocity of particles carried along in a streaming fluid was also measured. This technique is now incorporated in a commercial instrument by Brown Instrument Company for application to biology and fluid mechanics.

The first investigation of the time dependence of critical opalescence was performed with the study of a binary mixture, aniline-cyclohexane. The critical opalescence of pure carbon dioxide was next studied. The main result of that study was particularly interesting because it showed what few expected — namely, that the thermal conductivity of a pure fluid diverges at its critical point as a power of the temperature interval

56

from the critical temperature. This is an important constraint
in the formulation of theories of transport processes near crit-
ical phase transition. Much work of this kind is continuing in
other laboratories.

Coherent Scattering—Thermodynamic Data

A unique design feature of the interferometer developed
at CRL made it possible to observe light scattered at a small
angle in a vertical plane. This design was motivated by the
realization that by measuring downward refraction through a thin
vertical slab of fluid we should obtain the coefficient of com-
pressibility of the fluid. Since this coefficient diverges at
the critical point, we planned to locate the critical density
and temperature by refraction measurements. Our expectations
were correct but somewhat naive. Far above the critical tempera-
ture one observed the expected downward refraction, but as the
critical temperature was approached within a few hundredths of a
degree a beautiful interference pattern developed. From this
Fraunhofer pattern we learned how to extract a wealth of new
information. We found that the inverse compressibility of the
fluid on the critical isochore vanished according to

$$\frac{d\mu^*}{d\rho^*} = 28.57 \; \epsilon^{1.28} \text{ (dimensionless units)}$$

over four decades in $\epsilon = \Delta T / T_c$. Below the critical temperature,
at the liquid-vapor boundary, the inverse compressibility van-
ishes according to

$$\frac{d\mu^*}{d\rho^*} = 141 \; (-\epsilon)^{1.28} \qquad .$$

Below the critical temperature, the liquid-vapor density differ-
ence vanishes according to

$$\frac{\rho_{liquid} - \rho_{vapor}}{\rho_{crit}} = 3.53 [-\epsilon]^{0.346}$$

57

over four decades in ε. We found that these three quantities all vanish at the same temperature within 0.0002% (~0.6 millidegree C). For these measurements, development of precise thermostatic control was essential. At the conclusion of the experiments, we were able to hold a set temperature within 0.1 millidegree for many hours.

The Fraunhofer pattern at $T = T_c$ is determined by the shape of the critical isotherm $\mu = \mu(\rho, T_c) \to A\rho^\delta$. Our data determine A and δ, but the computations needed to extract these parameters are not completed.

Xenon appears to be a good candidate for the prototypical critical phase transition. As such, it repays painstaking study. The value of our optical determinations is enhanced by a painstaking analysis of older work which is being carried on at the National Bureau of Standards. In so far as the principle of corresponding states holds, the result for xenon applies to all nonpolar gases.

Outlook

Though the project at the Columbia Radiation Laboratory is ended, ideas generated here continue to lead a vigorous existence elsewhere. Laser optical measurements will continue for some time to reveal the static and transport properties of materials around critical points. Presently, many experimental programs are being initiated. Particularly interesting to us are the similarities and dissimilarities between the various critical transitions. Are the anomalies well described by power laws? If so, what are the precise values for the exponents; are they the same for all systems? What general properties of interactions are responsible for identical critical behavior in disparate systems? How valid is the idea that critical systems have one universal equation of state? Is that universal equation

derivable from the Lens-Ising model? Answers to such questions will be forthcoming in the next decade, and laser-optical measurements will play an important part.

III. SOLID STATE PHYSICS

A. INTERACTION BETWEEN A NEUTRAL BEAM AND A CONDUCTING SURFACE*
(P. Kusch, D. Raskin)

The ultra-high vacuum chambers described in the previous Progress Report[1] have been constructed (by Varian Associates, Palo Alto, Calif.) and are presently being tested at the factory. New instrumental components to be mounted in the ultra-high vacuum system have been designed.

After delivery of the vacuum system, the vacuum properties of the system will be tested with all components in place, and procedures to obtain the best vacuum under operating conditions will be determined. The beam producing, defining, and detecting components will then be aligned, and the experimental work on the deflection of neutral particles by a metal surface will be resumed.

An article describing the previous work on this experiment has been accepted for publication by The Physical Review.

(1) CRL Progress Report, April 30, 1968, p. 64.

B. EFFICIENCY OF IONIZATION ON METAL SURFACES*
(P. Kusch, A. Shih)

An experiment has been initiated to study the dependence of surface-ionization efficiency on the amplitude and the frequency of an applied oscillating electric field. We are interested mainly in the effect of electric fields of low amplitude (≈ 0.1 V/cm). The detection system consists of a large cathode (0.4 in. diam) within a cylindrical collector. This geometry allows the application of a small electric field to the ionization surface while a substantial potential difference between the cathode and collector is maintained.

The background noise from the molybdenum ionization sur-
face was originally very large because of the large cathode area.
A modification in which only the central part of the cylinder
served as collector and the complementary area acted as a guard
ring provided some reduction in noise. Further reduction was
obtained by baking out the cathode at a high temperature.

C. ADIABATIC DEMAGNETIZATION IN THE ROTATING FRAME*
   (S. R. Hartmann, D. Tse)

Research on this project has been completed, and the re-
sults are being prepared for publication.

D. NUCLEAR MAGNETIC RESONANCE IN FINE PARTICLES*
   (S. R. Hartmann, G. R. Mather)

None of our observations of the NMR's from the 100-Å and
20-Å platinum samples suggest that these samples behave like
collections of fine particles whose conduction electron levels
are quantized. Because signal-to-noise ratios were in all cases
poor, it is possible that some of the details of the NMR proper-
ties were obscured; nevertheless, the gross features of the data
(including the Knight shifts and spin-lattice relaxation rates)
are more suggestive of bulk-metal than fine-particle behavior.

The precise interpretation of our data is not at all clear
at this point, but in order to account for the fact that at low
temperatures (T $\approx$ 1.5°K) the 20-Å sample behaves rather like bulk
platinum, it would seem to be necessary to postulate the exist-
ence of an interaction which broadens the conduction band levels
by an amount greater than their average separation. Estimates

indicate that while none of the more obvious interactions are sufficiently effective to smear the conduction band of a 20-Å particle into a continuum, there is one mechanism that may possibly be far more effective than the others; this is the spin-flip scattering of electrons off lattice defects in the surface regions of the particles, a process which can take place because of the coupling of the electron spin to the translational degrees of freedom via the spin-orbit interaction. Using the expressions of Elliott[1] and Dyson[2] for the interaction time, and assuming that the electron is scattered each time it traverses the particle, we arrive at an estimate of $\Delta \varepsilon \approx 10^{-16}$ erg for the lifetime broadening of the electronic levels of 20-Å platinum particles. This is considerably smaller than the average level separation of $\delta \approx 4 \times 10^{-15}$ erg, but it is possible that our estimate is low because of the crudeness of the calculation. In any event, if the level broadening is intimately related to such a mechanism, then our failure to observe the expected fine-particle effects in platinum may result from the relatively large spin-orbit force in this metal.

It is possible to understand some of our data in a qualitative way if, in addition to level broadening, we assume that the electronic state density at the Fermi surface varies from particle to particle and that the lattice of each particle is badly distorted; in view of the smallness of the particles, such assumptions may not be unreasonable. However, there seems to be little of physical interest in such an interpretation, and for this reason we regard further experimental and theoretical work on the platinum samples to be of little value at this point. The problem of interest is the apparent necessity for assuming broadening of the electron levels in fine-particle platinum, for if this is a condition prevalent in all metals, fine-particle effects of the sort we hope to see may not be observable at all.

62